

CHEMICAL ALTERATION OF OIL WELL CEMENT WITH BASALT
ADDITIVE DURING CARBON STORAGE APPLICATION

A THESIS SUBMITTED TO
THE GRADUATE SCHOOL OF NATURAL AND APPLIED SCIENCES
OF
MIDDLE EAST TECHNICAL UNIVERSITY

BY

KAHILA MOKHTARI JADID

IN PARTIAL FULFILLMENT OF THE REQUIREMENTS
FOR
THE DEGREE OF MASTER OF SCIENCE
IN
PETROLEUM AND NATURAL GAS ENGINEERING

DECEMBER 2011

Approval of the thesis:

**CHEMICAL ALTERATION OF OIL WELL CEMENT WITH BASALT
ADDITIVE DURING CARBON STORAGE APPLICATION**

Submitted by **KAHILA MOKHTARI JADID** in partial fulfillment of the requirements for the degree of **Master of Science in Petroleum and Natural Gas Engineering Department, Middle East Technical University** by,

Prof. Dr. Canan Özgen
Dean, Graduate School of **Natural and Applied Sciences** _____

Prof. Dr. Mahmut Parlaktuna
Head of Department, **Petroleum and Natural Gas Engineering** _____

Prof. Dr. Ender Okandan
Supervisor, **Petroleum and Natural Gas Engineering Dept., METU** _____

Examining Committee Members

Prof. Dr. Mahmut Parlaktuna
Petroleum and Natural Gas Engineering Dept., METU _____

Prof. Dr. Ender Okandan
Petroleum and Natural Gas Engineering Dept., METU _____

Prof. Dr. Nilgün Güleç
Geological Engineering Dept., METU _____

Assist. Prof. Dr. Çağlar Sınayuç
Petroleum and Natural Gas Engineering Dept., METU _____

M.Sc. Güray Karakaya
TPAO, ANKARA _____

Date: 20/12/2011

I hereby declare that all information in this document has been obtained and presented in accordance with academic rules and ethical conduct. I also declare that, as required by these rules and conduct, I have fully cited and referenced all material and results that are not original to this work.

Name, Last name : Kahila Mokhtari Jadid

Signature :

ABSTRACT

CHEMICAL ALTERATION OF OIL WELL CEMENT WITH BASALT ADDITIVE DURING CARBON STORAGE APPLICATION

Mokhtari Jadid, Kahila

M.Sc., Department of Petroleum and Natural Gas Engineering

Supervisor: Prof. Dr. Ender Okandan

December 2011, 96 pages

Capturing and storing carbon dioxide (CO₂) underground for thousands of years is one way to reduce atmospheric greenhouse gases, often associated with global warming. Leakage of CO₂ through wells is one of the major concerns when storing CO₂ in depleted oil and gas reservoirs. CO₂-injection candidates could be new wells, or old wells that are active, closed or abandoned.

To prevent the leakage, the possible leakage paths and the mechanisms triggering these paths must be examined and identified. It is known that the leakage paths can occur due to CO₂-rock interaction and CO₂-water-cement interaction.

Interaction between well cement and carbon dioxide has attracted much renewed interest because of its implication in geological storage of carbon dioxide. The diffusion of CO₂-water through well cement is a long-term phenomenon which can take many thousand years. Partial pressure, porosity, permeability, cement type, moisture content and temperature are the factors that affect the carbonation of well cement. The objective of this research is to investigate the chemical reactions of the

dissolved CO₂ in the synthetic formation water with the plugs of well cement. Cement specimens were left in contact with CO₂ saturated brine at 1100 psi and 65 °C for three months. The 1100 psi pressure and 65 °C temperature are the points where CO₂ is in the state of CO₂ saturated brine. The four cement plugs studied differed in their basalt content from 0%, 6%, 9%, and 13% by whole mix weight. The effects of basalt content studied are change in porosity, permeability and compressive strength. The scanning electron microscope images were obtained to observe the depth of penetration of CO₂-brine solution into cement plugs after three months of contact. The results indicate that presence of basalt increased the compressive strength of plugs and decreased porosity and permeability. As a conclusion the use of basalt as an additive to well cement can be beneficial in CO₂ storage wells.

Keywords: CO₂ storage, CO₂ saturated brine, CO₂-water-cement-interaction, basalt, SEM.

ÖZ

KARBON DEPOLAMA UYGULAMALARINDA BAZALT KATKILI KUYU ÇİMENTOLARININ KİMYASAL DEĞİŞİMİ

Mokhtari Jadid, Kahila

Yüksek Lisans, Petrol ve Doğal Gaz Mühendisliği Bölümü

Tez Yöneticisi: Prof. Dr. Ender Okandan

Aralık 2011, 96 sayfa

Karbondioksitin yakalanması ve yeraltında binlerce yıl depolanması, atmosferdeki sera gazlarının azaltılması için bir yoldur. Bu da küresel ısınma ile doğrudan ilgilidir. CO₂'in terk edilen petrol ve gaz kuyularından sızması önemli sorunlardan biridir. Yeni, kapalı veya terk edilmiş kuyular CO₂ enjeksiyonu için aday olabilir.

Kaçığı engellemek için, olası sızıntı yolları ve tetikleme mekanizmaları incelenmeli ve tespit edilmelidir. Bu kaçak yollarının CO₂-kayaç ve CO₂-su çimento etkileşimleri nedeniyle olabileceği bilinmektedir.

Çimento ve CO₂ arasındaki etkileşim, karbondioksitin jeolojik depolanması nedeniyle çok ilgi çekmektedir. CO₂-suyun kuyu çimentosuna difüzyonu binlerce yıl sürebilen uzun vadeli bir olgudur. Kısmi basınç, gözeneklilik, geçirgenlik, çimento tipi, nem içeriği ve sıcaklık çimento karbonasyonunu etkileyen faktörlerdir. Bu çalışmanın amacı, sentetik su içinde çözünmüş olan CO₂'in çimento karot örnekleriyle olan kimyasal reaksiyonlarını tespit etmektir. Çimento örnekleri, 1100 psi ve 65 °C de üç ay boyunca CO₂ ile doymuş tuzlu suya temas halinde bekletildi. Bazalt katkılı çimento karot örnekleri içerisinde, ağırlıkça %0, %6, %9 ve %13 bazalt olacak şekilde hazırlandı. Bazalt içeriğinin etkisi gözeneklilik, geçirgenlik ve

basınç dayanımı açısından incelendi. Penetrasyon derinliğini görmek için CO₂-tuzlu suya üç ay boyunca maruz bırakılan çimento örneklerinin taramalı elektron mikroskobu görüntüleri elde edildi. Sonuçlar, bazalt içeren örneklerin basınç dayanımının arttığı ve gözeneklilik, geçirgenlik değerlerinin azaldığını göstermiştir. Sonuç olarak, bazaltın CO₂ depolama kuyularının çimentolarında katkı maddesi olarak kullanımı yararlı olabilir.

Anahtar Kelimeler: CO₂ depolama, CO₂ doymuş tuzlu su, CO₂-su-çimento etkileşimi, bazalt, SEM.

To my parents

ACKNOWLEDGMENTS

This dissertation would not have been possible without the support from mentors, family, friends, the Department of Petroleum and Natural Gas Engineering.

Firstly and foremost, I would like to express my deepest and sincere thankfulness to my thesis supervisor Prof. Dr. Ender Okandan not only for her guidance, advice, criticism, encouragement, support and precious insight throughout the research but also her unforgettable and valuable contribution to my career. She was beyond being the advisor and professor for these years.

I also thank Prof. Dr. Mahmut Parlaktuna, the chairperson of Department of Petroleum and Natural Gas Engineering, for his endless support and valuable advice. Also my special thanks go to my thesis committee members for their valuable suggestions and comments.

I would like to thank to my dear friends, Sevtac Bulbul and Guray Karakaya for their endless support, encouragement and love and also my other friends for their understanding, friendship and love.

Naci Dogru is also deeply acknowledged for constructing and helping during the experimental set up.

Turkish Petroleum Corporation is greatly appreciated for providing the cement plugs and also for their analysis and support.

I wish to thank the Departments of Geological Engineering, Metallurgical Engineering for the mineralogical and SEM analyses.

At last but not least, I would like to thank my parents Mohammadreza and Shahin for their never ending support, trust love and encouragement and my special thanks go to my mother who always was supportive, kind and so patient during my thesis work. This study is simply impossible without her.

TABLE OF CONTENTS

ABSTRACT.....	iv
ÖZ.....	vi
TABLE OF CONTENTS.....	x
LIST OF FIGURES	xiii
LIST OF TABLES	xv
CHAPTERS	
1. INTRODUCTION	1
1.1. Carbon Capture and Storage	2
1.2. Geological storage of CO ₂	3
1.2.1. Source examples of CO ₂ Storage Sites	4
2. LITERATURE SURVEY	8
3. THEORY	12
3.1. Well cementing	12
3.2. Well integrity	13
3.3. Portland cement properties and categories.....	14
3.3.1. Portland cement composition.....	14
3.4. Oil well cement properties and categories	16
3.4.1. Characteristics and Manufacturing process of oil well cements.....	16
3.4.2. Oil well cement grades and types	16
3.5. Cement-CO ₂ -brine interaction in wellbore Environment	19
3.6. Solubility of carbon dioxide in water.....	19
3.7. Diffusion of CO ₂ through cement	22
3.8. Three chemical reactions due to cement-CO ₂ -brine interaction	22
3.9. Basalt.....	24
3.9.1. CO ₂ -water -basalt interaction.....	24
3.9.2. In situ mineral carbonation in basaltic rocks	25

4. STATEMENT OF THE PROBLEM	27
5. EXPERIMENTAL PROCEDURE AND SET UP	28
5.1. Material used in experiment.....	28
5.2. Cement slurry preparation.....	30
5.3. Experimental set up.....	35
5.4. Experimental Procedure.....	38
5.5. Amount of CO ₂ used in experiment.....	39
6. RESULTS AND DISCUSSION	43
6.1. Synthetic formation water analysis results of four samples.....	43
6.2. Permeability and porosity measurement of cement plugs before CO ₂ brine treatment.....	44
6.3. Permeability and porosity measurement of cement plugs after CO ₂ brine treatment.....	45
6.4. Compressive strength analysis of cement plugs	47
6.5. SEM analysis	49
7. CONCLUSION.....	53
REFERENCES.....	55
APPENDICES	57
A. PORTLAND CEMENT TYPES.....	57
A.1 European Standards (EN197-1) Portland cement type and composition.....	57
A.2 American Standards (ASTM C150) Portland cement type and composition	58
B. OIL WELL CEMENT.....	61
C. MIXING DEVICES FOR PREPARATION CEMENT PLUGS.....	68
C.1 Procedures	69
C.1.1. Temperature of water and cement.....	69
C.1.2. Mix water	69
C.1.3. Mixing quantities.....	69
C.1.4. Mixing cement and water.....	69
D. PHOTOGRAPHS OF CEMENT PLUGS AND EXPERIMENTAL SET-UP.....	70
E. COMPARSION GRAPHS OF ELEMENT CONCENTRATION IN CO ₂ - WATER MIX AND FOUR CEMENTPLUGS	72

F. POROSITY AND PERMEABILITY MEASUREMENT APPARATUS OF CEMENT PLUGS ACCORDING TO THE API RP 40	74
F.1. Boyle,s law double-cell method for grain volume (Porosity Determination).....	74
F.1.2. Apparatus and Procedure	74
F.2. Boyle,s law single cell method for direct pore volume	75
F.2.1.Apparatus and Procedure	75
F.3. Axial, Steady-State flow of gases (Permeability determination).....	76
G. AP-1000 VERSA-TESTER APPARATUS FOR MEASURING THE	
COMPRESSIVE STRENGTH OF CEMENT PLUGS	79
H. PHOTOGRAPHS OF CEMENT PLUGS AFTER 90 DAYS EXPERIMENT ...	80
I. SEM/EDS ANALYSIS OF FOUR CEMENT PLUGS BEFORE AND AFTER EXPERIMENT	83

LIST OF FIGURES

FIGURES

Fig1.1 Comulative world carbon dioxide emissions.....	2
Fig 1.2 74 CCS projects across the world in 2011.....	4
Fig 3.1 An abandoned well leakage pathways.....	13
Fig 3.2 Solubility of carbon dioxide in water (temperature, pressure effects).....	21
Fig 5.1 Compressive strength of sample#1	32
Fig 5.2 Compressive strength of sample#2	33
Fig 5.3 Compressive strength of sample# 3	33
Fig 5.4 Compressive strength of sample# 4.....	34
Fig 5.5 The schematic diagram of the experimental set-up.....	36
Fig 5.6 Pressure and temperature recordings of experiment.....	41
Fig 5.7 Carbon dioxide phase diagram	42
Fig 6.1 Cement plug 4 while applying vertical load.....	48
Fig 6.2 SEM surface image of cement plug 1 after 3 months CO ₂ treatment.....	50
Fig 6.3 SEM surface image of cement plug 2 after 3 months CO ₂ treatment.....	50
Fig 6.4 SEM surface image of cement plug 3 after 3 months CO ₂ treatment.....	51
Fig A.1 European standards portland cement type and compositions	57
Fig C.1 Examples of typical cement mixing devices.....	68
Fig D.1 Photograph of 4 samples.....	70
Fig D.2 Photograph of 4 cement plugs with different compositions before 90 days. 70	70
Fig D.3 Photograph of 4 cement plugs with four core holders	71
Fig D.4 Photograph of experimental set up	71
Fig E.1 Na concentration variation from cement plugs 1~4.....	72
Fig E.2 K concentration variation from cement plugs 1~4.....	72
Fig E.3 Mg concentration variation from cement plugs 1~4	73
Fig E.4 Ca concentration variation from cement plugs 1~4	73
Fig F.1 Double-Cell Boyles's Law Porosimeter.....	74
Fig F.2 Schematic of isostatic load cell for direct pore volume determination	75
Fig F.3 Schematic of Permeability Apparatus for Axial Flow of Gas.....	77
Fig F.4 Simplified Flow Diagram for Low Pressure, Axial gas Flow Permeability..	78
Fig G.1 Schematic of Versa-Tester Apparatus.	79

Fig H.1 Photograph of cement plugs after experiment	80
Fig H.2 Photograph of cement plug 1 after experiment.....	80
Fig H.3 Photograph of cement plug 2 after experiment.....	81
Fig H.4 Photograph of cement plug 3 after experiment.....	81
Fig H.5 Photograph of cement plug 4 after experiment.....	82
Fig I.1 Near to surface view of sample #1 (before EXP)	83
Fig I.2 Near to surface view of sample #1(after EXP)	83
Fig I.3 Near to surface view of sample #2 (before EXP)	84
Fig I.4 Near to surface view of sample #2 (after EXP)	84
Fig I.5 Near to surface view of sample #3 (before EXP)	85
Fig I.6 Near to surface view of sample #3 (after EXP)	85
Fig I.7 Near to surface view of sample #4 (before EXP)	86
Fig I.8 Near to surface view of sample #4 (after EXP)	86
Fig I.9 Inner view of in depth SEM analysis for sample #1(after EXP)	87
Fig I.10 Inner view of in depth SEM analysis for sample #2(after EXP)	87
Fig I.11 Inner view of in depth SEM analysis for sample #3(after EXP)	88
Fig I.12 Inner view of in depth SEM analysis for sample #4(after EXP)	88
Fig I.13 SEM/EDS micrograph of near surface of sample#1(after EXP)	89
Fig I.14 SEM/EDS micrograph for inner section of sample #1(after EXP).....	90
Fig I.15 SEM/EDS micrograph of near surface of sample #2(after EXP)	91
Fig I.16 SEM/EDS micrograph for inner section of sample #2(after EXP).....	92
Fig I.17 SEM/EDS micrograph of near surface of sample #3(after EXP)	93
Fig I.18 SEM/EDS micrograph for inner section of sample #3(after EXP).....	94
Fig I.19 SEM/EDS micrograph of near surface of sample #4(after EXP)	95
Fig I.20 SEM/EDS micrograph for inner section of sample #4(after EXP).....	96

LIST OF TABLES

TABLES

Table 1.1 Global potential estimation for CO ₂ storage.....	3
Table 3.1 Typical composition and properties of API classes of Portland cement ...	18
Table 5.1 Chemical composition of class G cement.....	28
Table 5.2 Chemical properties of Class G cement.....	29
Table 5.3 Physical properties of Class G cement.....	29
Table 5.4 Chemical compositions of basalt used in experiment.....	29
Table 5.5 Synthetic water analysis.....	30
Table 5.6 Cement slurry compositions	31
Table 5.7 Class G cement quality control results.....	31
Table 5.8 Compressive strength of 4 cement plugs	34
Table 5.9 Experimental apparatus and technical specification	37
Table 6.1 Synthetic formation water result.....	43
Table 6.2 Porosity, permeability values of four cement plugs before CO ₂ injection ..	45
Table 6.3 Porosity, permeability values of four cement plugs after CO ₂ injection	46
Table 6.4 Compressive strength of 4 plugs before CO ₂ saturated brine treatment.....	47
Table 6.5 Compressive strength of 4 plugs after CO ₂ saturated brine treatment.....	48
Table A.1 Type of Portland cement	58
Table A.2 Portland cement mechanical and physical requirements	59
Table A.3 Portland cement chemical requirements	60
Table B.1 Applications of API classes of cement.....	61
Table B.2 Ordinary type (O).....	62
Table B.3 Moderate sulfate-resistant type (MSR)	63
Table B.4 High sulfate-resistant type (HSR)	64
Table B.5 Physical requirements for API cements	65
Table B.6 Minimum compressive strength after 8 h curing time	66
Table B.7 Minimum compressive strength after 24 h curing time	67
Table C.1 Slurry component quantities.....	69
Table F.1 Porosity measurement of cement plugs before and after experiment.....	76

Table F.2 Porosity measurement of cement plugs before and after experiment.....	78
Table I.1 Element analysis of near to surface of sample # 1 (before EXP).....	83
Table I.2 Element analysis of near to surface of sample # 1 (after EXP).....	83
Table I.3 Element analysis of near to surface of sample # 2 (before EXP).....	84
Table I.4 Element analysis of near to surface of sample # 2 (after EXP).....	84
Table I.5 Element analysis of near to surface of sample # 3 (before EXP).....	85
Table I.6 Element analysis of near to surface of sample # 3 (after EXP).....	85
Table I.7 Element analysis of near to surface of sample # 4 (before EXP).....	86
Table I.8 Element analysis of near to surface of sample # 4 (after EXP).....	86
Table I.9 SEM/EDS element analysis of near to surface of sample # 1(after EXP) ..	89
Table I.10 SEM/EDS element analysis for inner section of sample # 1(after EXP) ..	90
Table I.11 SEM/EDS element analysis of near to surface of sample # 2(after EXP)	91
Table I.12 SEM/EDS element analysis for inner section of sample # 2(after EXP) ..	92
Table I.13 SEM/EDS element analysis of near to surface of sample # 3(after EXP)	93
Table I.14 SEM/EDS element analysis for inner section of sample# 3(after EXP) ...	94
Table I.15 SEM/EDS element analysis of near to surface of sample # 4(after EXP)	95
Table I.16 SEM/EDS element analysis for inner section of sample # 4(after EXP) ..	96

NOMENCLATURE

API	American Petroleum Institute
ASTM	American Society of Testing Materials
Bc	Burden of consistency
CCS	Carbon Capture & Storage
CFR	Cement Friction Reducer
EOR	Enhanced Oil Recovery
HSR	High Sulfate Resistant
MSR	Moderate Sulfate Resistant
P	Pressure
R	Universal gas constant
SEM	Scanning Electron Microscope
T	Temperature
V	Volume
XRD	X-Ray Diffraction

CHAPTER 1

INTRODUCTION

In the 1980s the consensus position formed in UN conferences on climate change that human activity was causing carbon dioxide levels to increase which is leading to the beginning of the modern period of global warming. Climate change is considerable and continuous change in the statistical distribution of weather patterns over time periods from decades to millions of years. Change in humidity, glacier melting, sea level rise, increase in heat content of ocean, increase temperature over land and over oceans are the main indicators of climate change. One of the main causes of global warming is human activities mainly due to burning of fossil fuels. In addition to these natural events also effect the rise of Earth's average temperature; these events are volcanic activities and variations in Earth's orbit.

The main source of CO₂ emissions come from use of fossil fuels in transportation, industrial plants, refineries and thermal power plants. Emission from transportation can be reduced by changing the design of motors and also by changing the quality of fuels. The emissions resulting from industrial activities can be reduced by increasing efficiency; producing the products with less fuel. However even after all these activities, there will be CO₂ emitted to the atmosphere. The ultimate elimination of CO₂ emission will be possible by storing CO₂ underground in geological formations where it will be trapped for millions of years.

Fig 1.1 shows the fossil and Industrial CO₂ emissions as Gigatons of CO₂ per year in different countries from 1990 to 2095. Africa, Middle East, Latin America, Southeast Asia, India and China are the countries where increase of CO₂ emissions will be higher until 2095 year. The chart consists of two parts; Annex I and Non-Annex I. Annex I part shows the developed countries, CO₂ emissions while Non-Annex I

shows the CO₂ emissions in developing countries. Approximately 90% of the growth in global emissions in the remainder of this century is projected to occur in developing (“Non-Annex I”) countries.

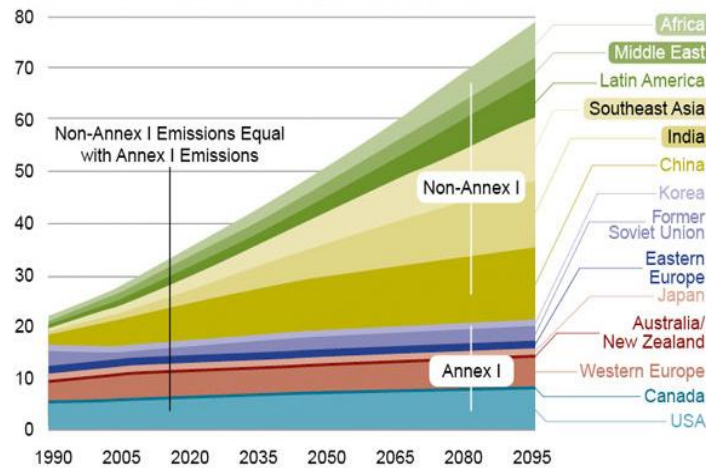


Fig 1.1 Cumulative world carbon dioxide emissions (1)

1.1 Carbon Capture and Storage

Large amount of emission of CO₂ to the atmosphere due to human activities and natural events caused many concerns regarding climate change, so carbon capture and storage, represents one possible approach for stabilizing greenhouse gas. Carbon capture and storage, as the name implies, consist of three stages which are capture, transport and long-term storage of carbon dioxide in underground geological formation such as deep saline aquifers, oil and gas fields, basalt formations and unmineable coal seams.

First of all, carbon capture and storage starts with carbon capture which is capturing CO₂ from emission of thermal power stations, industrial sites. Capturing process can be done by three different technologies post combustion, pre combustion and oxyfuel. Secondly, CO₂ is transported by pipelines to the suitable underground storage sites and finally CO₂ is injected and stored in underground structures. The main priority of carbon dioxide storage is to have a reliable, safe and long-term storage capacity of the formation where it is stored.

1.2 Geological storage of CO₂

CO₂ emitted by large sources like industrial plants and thermal power plants could be captured and stored in depleted oil and gas fields, coal seams and deep saline reservoirs. The IEA Greenhouse Gas R&D program reports the estimated global potential for CO₂ storage in geological reservoirs.(2)

Table 1.1 Global potential estimation for CO₂ storage (2)

Geological Storage Option	Global Capacity	
	Giga tons of CO ₂	As a proportion of total emissions 2000 to 2050
Depleted oil and gas fields	920	45%
Unminable coal seams	>15	>1%
Deep saline reservoirs	400-10,000	20-500%

The comparisons in the table above show that geological storage could have an essential impact on CO₂emissions. In the early 1990s, the estimation for deep saline reservoirs were made which in Northwest Europe the storage capacity could be as high as 800 Giga tons CO₂.(2). There are 74 large-scale integrated CCS projects around the world14 projects are either in operation or construction and have a total CO₂ storage capacity of over 33 million tons a year. Fig 1.2 indicates 74 CCS projects across the world in 2011.(3)

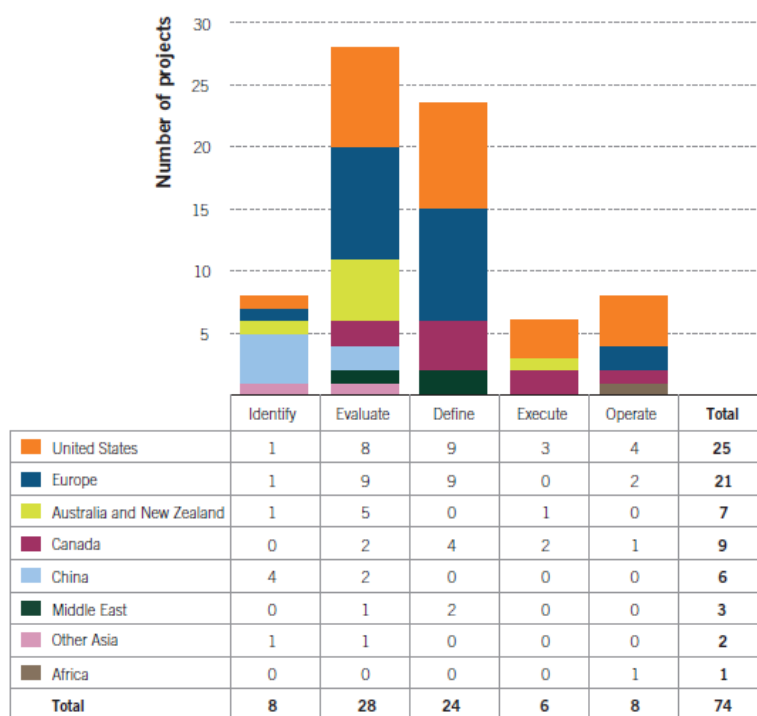


Fig 1.2 74 CCS projects across the world in 2011 (3)

The four main storage sites range from aquifers beneath quite deep gas fields (e.g. In Salah in Algeria, Snohvit in Norway) to the much shallower Utsira aquifer (e.g. Sleipner in Norway) and the on land shallow saltwater-filled, porous rocks formations (e.g. Ketzin Germany). Other sites include an enhanced oil recovery project (Weyburn in Canada), an old gas field (K12-B in The Netherlands) and an enhanced coalbed methane project (e.g. Kaniow in Poland).

1.2.1 Source examples from CO₂ storage sites

In Salah – Algeria

In Salah, an industrial-scale CCS project in Algeria has been in operation since 2004. More than three million tons of CO₂, separated during gas production, have been securely stored in a deep saline aquifer. BP, Sonatrach and Statoil, the project operators, aim to store a total of 17 million tons over the next 20 years. The In Salah project is of global significance; providing assurance that secure industrial-scale geological storage of CO₂ is a viable option for climate change mitigation. The project is supported by the US Department of Energy and the EU. The Carbon

Sequestration Leadership Forum has identified In Salah as one of the most important industrial-scale CCS initiatives globally – helping to counter the view that the technology is not yet proven.(4)

Sleipner - Norway

Sleipner site operator is Statoil Hydro and CO₂ storage operation started in 1996. The project started under the auspices of the Saline Aquifer CO₂ Storage (SACS) research and development project. The operator found that it is easier as well as more economical to separate the CO₂ (4 to 9.5 % in content) from the natural gas and re-inject it instead of paying a CO₂ tax. The removed CO₂ is injected into salt water containing sand layer, called the Utsira formation, which lies 1000 meter below sea bottom. Sleipner site is the large scale demonstration of storage with more than 7 million tons of CO₂ in situ during 2008. (4)

Ketzin - Germany

Under the management of the GFZ in cooperation with 18 partners from nine countries, the injection and storage of CO₂ in deep, saltwater-filled, porous rocks is studied on an onshore site in Europe. It is accepted as a test site where extensive monitoring, geochemical and geophysical research are conducted. The project aims to store up to 60,000 tons of CO₂ in a saline aquifer at a depth of more than 600 m. An injection well and two observation wells have been successfully drilled to depths of 800 m. The project involves intensive monitoring of the injected CO₂ using a broad range of geophysical and geochemical techniques.(4)

Weyburn - Canada

The Weyburn oil field operator is EnCana Corporation and lies on the northwestern rim of the Williston Basin, 16 km south east of Weyburn. A Canadian oil and gas corporation in 1998 announced to implement a large scale EOR project in an oilfield near Weyburn, Saskatchewan, using CO₂ captured from a coal gasification power plant. This provided a chance to demonstrate and study a large-scale geological storage project. The oil field started operation in 1954; there are about 650 production and water injection wells in operation. Average daily crude oil production is about

18,200 barrels. The field is in production decline, in order to keep the field viable CO₂ injection began in 2000. Now, the commercial oil recovery project is also a demonstration project for CO₂ storage in an oilfield.(4)

K12-B - The Netherlands

The K12-B gas field operator is Gaz de France and is located in the Dutch sector of the North Sea. K12-B is the first site in the world where CO₂ is being injected into the same reservoir from which it was, together with methane, produced. Investigated is the feasibility of CO₂ injection and storage in depleted natural gas field and the corresponding monitoring and verification. Since 1987, it has been producing natural gas with a relatively high CO₂ content. Prior to transport to shore, the CO₂ is separated from the natural gas. Until recently the CO₂ was vented and in 2004, CO₂ was injected into the gas field, at a depth of approximately 4000 m. In January 2009, the CO₂ injection was ongoing and since 2004 a total of 60,000tons of CO₂ has been injected in the nearly depleted gas field K12-B. (4)

Kaniow - Poland

The Kaniow field operator is CMI, a pilot site for CO₂ storage in coal seams. This site consisted of one injection and one production well. From August 2004 to June 2005 about 760 tons of CO₂ has been injected into the reservoir. A follow-up EC project aimed at determining the storage performance of the reservoir, i.e. whether the injected CO₂ was adsorbed onto the coal or whether it was still present as free gas in the pore space.(4)

The storage of CO₂ in geologic formations requires a thorough evaluation of potential leakage through wellbores which penetrate them.

During this study a three month experiment was carried out to determine the effect of CO₂ saturated brine exposure on wellbore cement at 1100 psi pressure and 65°C temperature. Class G cement which is an ordinary well cement, basalt, synthetic formation water and CFR (additive) mixed based on API classification and used for the experiments. Four cement plugs with different basalt contents were prepared and

then exposed to dissolved CO₂-saturated brine. The chemical reactions occurring from the analysis of water samples and SEM analysis were interpreted; their effects on compressive strength of plugs were studied.

CHAPTER 2

LITERATURE SURVEY

In three decades, the laboratory studies have shown that, over a long term, the pure well cement (Portland cement based) could not maintain the zonal isolation.

Onan (1984), investigated the supercritical CO₂ influence on cement and also the carbonation effect on the hydration process of cement. He concludes that after a long term exposure to the supercritical CO₂, the products which are formed by the Portland cement hydration shows decomposition into calcium carbonate and siliceous residue. Well cements that are in the exposure of a supercritical CO₂ in lower pressure and temperature condition demonstrated greater reactivity while increasing the pressure of CO₂ increased the reaction rate with no regard to the carbonation conditions.(5)

Barlet Gouedard et al. (2006 and 2009), carried out an experiment regarding geochemical alteration of Portland cement due to exposure to the CO₂ saturated brine and supercritical CO₂. Two materials processed conventional Portland cement and Schlumberger CO₂ resistant Cement (SCRC) .SCRC contains CO₂ inert particles and shows better CO₂resistance than conventional Portland cement. In the Portland cement under 90 °C and 280 bars after 6 months at the interface between CO₂ saturated brine and supercritical CO₂, spalling clearly has been observed. In contrast, the SCRC cement presents a homogenous pattern with a limited carbonation threshold. (6)

Barbara G.Kutchko (2007), conducted experiment to assess the well cements durability; the experiments showed a considerable variation in initial degradation (9 days of exposure) based on the curing conditions. The high pressure (30.0 Mpa) and

temperature (50 °C) curing environment increased the degree of hydration and caused a change in the distribution and microstructure of the $\text{Ca}(\text{OH})_2$ phase within the cement. Cement cured at 22 °C and 0.1 MPa. The cement cured at 50 °C and 30.3 MPa exhibited a shallower depth of degradation and displayed a well-defined carbonated zone as compared to cement cured under ambient condition. This is due to smaller, more evenly distributed $\text{Ca}(\text{OH})_2$ crystals that provide a uniform and effective barrier to CO_2 attack. at 50 °C and 30.3 MPa proved to be more resistant to carbonic acid attack than cement.(7)

Barbara G.Kutchko (2008), observed two different chemical alterations. Alteration of cement exposed to supercritical CO_2 was the same as the cement in contact with the atmospheric CO_2 which is an ordinary carbonation, while modification of cement exposed to CO_2 saturated brine was a typical attack of acid into cement. For 1 year, the extrapolation of hydrated cement alteration rate measured which demonstrates a range of penetration depth of 1.00 ± 0.07 mm for CO_2 saturated brine and 1.68 ± 0.24 mm for supercritical CO_2 after 30 years. The values penetration depths are consistent with field sample observations from an enhance oil recovery site under same pressure and temperature conditions after 30 years of exposure to CO_2 saturated brine.(8)

Barbara G.Kutchko (2009), carried out experiment to determine the mechanism and rate of reaction of pozzolan-amended class H Portland cement which exposed to CO_2 saturated brine and supercritical one. Types F fly ash, the pozzolan additive used in cement blends. The pozzolan –cement blends ratios of 35:65 and 65:35 were exposed to CO_2 . The rate of penetration in 65:35 mix is much faster than the 35:65 blend and the extrapolation of this rate for 35:65 showed a depth of penetration of 170-180 mm for both CO_2 supercritical and CO_2 saturated brine. In spite of modification in both pozzolan systems, the cement which reacted became impermeable to fluid flow after it is exposed to CO_2 saturated brine.(9)

Ashok Santra (2009), performed experiment regarding the role of pozzolanic supplements such as fly ash and silica fume in Portland cement blends. For several weeks, cement specimens kept under water at 2000 psi CO_2 pressure and 200 ° F.

The outcomes exhibit that the carbonation depth during 15 days at a given pressure and temperature is directly proportional to amount of pozzolanic materials.(10)

J.W. Carey (2009), proposes three hypotheses for the CO₂ carbonation: 1-migration along wellbore interfaces, 2- flow through cement and 3- diffusion from CO₂ bearing cap-rock. The numerical model indicates that supercritical CO₂ will not flow through good quality cement due to capillary properties of cement. In this case, leakage of CO₂ is confined to wellbore interfaces and carbonation of cement occurs by diffusion of CO₂ into the cement from the interface. In addition, carbonation by diffusion creates reaction fronts that are distinct from the uniform carbonation pattern generated by flow of CO₂ through cement. (11)

N. Gaurina Medimurec (2010), presented the flow pathways throughout the well, the behavior of CO₂ at reservoir condition, and geochemical alteration of well cement because of injection of supercritical CO₂. The chemical interactions between oil well cement and injected CO₂ could result in leakage due to degradation of cement. In CO₂ sequestration site, the most important issue in the well systems is the cement-formation interfaces and casing-cement integrity. He concluded that for reducing porosity, permeability and also reducing the Ca (OH) ₂ as well as changing the composition of C-S-H to more CO₂- resistive, it is better to lower the amount of Portland cement by adding pozzolanic and reactive supplementary materials.(12)

Koji, Takase (2010), presented that non Portland cements alone might not be useful and sufficient for well bore integrity for long term and as a solution, optimization of mechanical properties with non-Portland cement for well bore integrity are recommended for CCS wells. By carrying out well cement integrity and temperature analysis, the cement sheaths are designed by well construction team to withstand operations of well for the life of wellbores.(13)

R. Felicetti (2001) ascertained the feasibility of randomly distributed basalt fiber reinforcement to improve the fracture toughness of oil well cement slurries. Nine types of slurries reinforced with fibers of different lengths and contents were tested for rheological and mechanical performance. Test result showed that an appropriate

choice of fiber volume and length can noticeably increase fracture toughness of cement matrix, without appreciably impairing the slurry's rheological properties.(14)

Sigurdur Reynir Gislason (2009) described the kinetic and thermodynamic basis for mineral storage of CO₂ in basaltic rock and also the optimization of this storage. Dissolution of carbon dioxide into aqueous phase is facilitated the mineral storage and the amount of water needed for the dissolution decreases with decreased salinity, temperature and increased pressure. The rate of release of cations from silicate minerals and glasses is the factor which restricting the mineral fixation rate of carbon in silicate rocks. Basalts and ultramafic rocks, in glassy state, which have high concentration of cations, fast dissolution rate and abundance at surface, are most favorable rock kinds for mineral sequestration of CO₂. The CarbFix project optimize and develop technology for in situ mineralization of carbon into basalts. CarbFix consists of laboratory experiments, natural analogue studies, injection of CO₂ water into basaltic rocks and geochemical modeling. The injection site is situated about 3 km south of the Hellisheidi geothermal power plant in south west of Iceland. In basaltic rocks the surface area and large reservoir volume within relatively rapid CO₂-water-rock reactions may permit for permanent and safe geologic storage of carbon dioxide.(15)

CHAPTER 3

THEORY

CO₂ injected into geologic formations for underground storage will dissolve into formation water and form carbonic acid at different pH levels depending on salinity of formation water. The concentration of carbonic acid in the formation is critical for cementing CO₂ storage wells. The cement used in well cementing job should have long-term mechanical resiliency against the carbonic acid. Use of proper cement mix might be sufficient for long term wellbore integrity.

3.1 Well cementing

Cementing is the process, which consists of mixing water, cement slurry and additives pumping down through casing, into the annulus between the wall of the well and casing. Two main functions of this process are to confine fluid movements between formations and to support the casing. There are two important cementing activities; liner cementing or cementing the casing, which is called primary cementing and it is one of the most important operations in oil and gas well development. Squeeze cementing and plug cementing are the other cementing operations denoted as secondary or remedial cementing. Cement also contributes to the protection of casing corrosion and in deep drilling operation in the protection of casing from loads. Materials of well cementing are different from Portland cement used in civil engineering constructions. For oil well cementing the widely used ones are Portland type cements. The oil well cements, which can be used both in offshore platforms and onshore fields are subjected to wide ranges of temperatures and pressures. American Petroleum Institute (API) provides eight classes of oil well

cements based on depths. In section 3.4 the types and grades of oil well cement are mentioned.(16)

3.2 Well integrity

The loss of well integrity has been identified as the biggest risk helping to CO₂ leakage from underground storage sites. Wellbores represent the most likely route for leakage of CO₂ from geologic carbon storage. Abandoned wells are typically sealed with cement plugs intended to block vertical migration of fluids. In addition, active wells are usually lined with steel casing, with cement filling the outer annulus in order to prevent leakage between the casing and formation rock.

There are several leakage pathways which can take place along abandoned wells and/or cased holes as shown in below Figure 3.1.

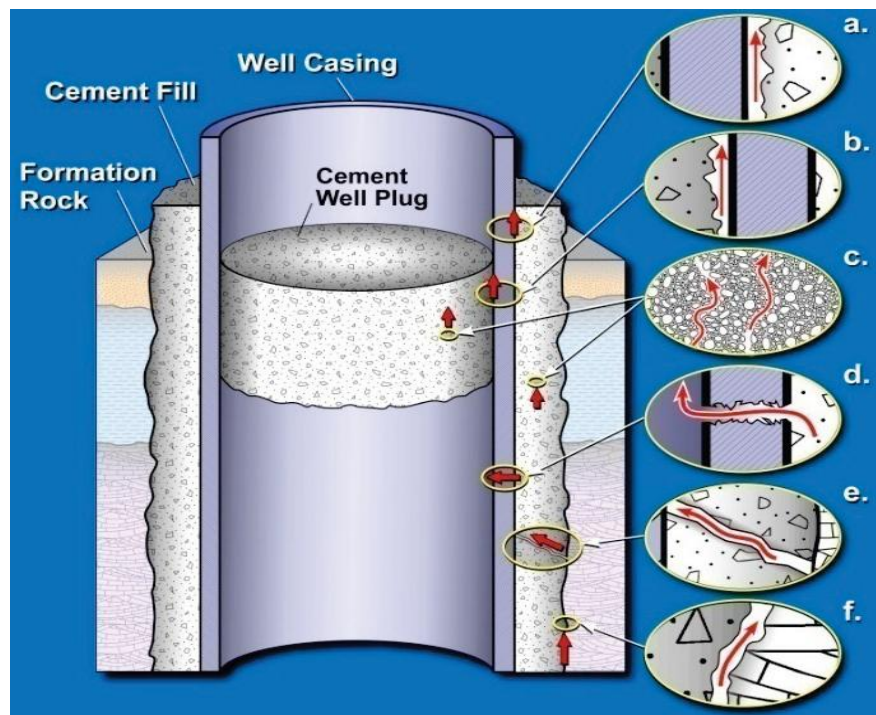


Fig 3.1 An abandoned well leakage pathways (12)

The leakage pathways can be between the cement and outside of the casing (3a), between the inside of the casing and cement (3b), through the cement plug

(3c), through the corrosion of the casing (3d) , through cement fractures in the annulus (3e) and leakage can be between cement and formation in the region of annular (3f). For identifying how the cement is effective against the fluid leakage, the determination of the integrity and permeability of the cement in abandoned well and in annulus are required. In long term CO₂ storage at reservoir condition the cement with low permeability is more sufficient.(12)

3.3 Portland cement properties and categories

Portland cement is fine powder obtained from grinding clinker Portland cement and fewer amounts of calcium sulfate and up to 5% minor constituent (fly ash, silica fume). Calcium, silica, alumina, iron are the primary components of raw materials for Portland cement. The raw materials are mixture of argillaceous (alumina and silica) material like shale, clay, blast furnace slag and fly ash and limestone. Portland cement is used in production of concrete, which is a composite material, contains aggregate (gravel and sand), cement and water. Concrete as a construction material can be formed in any shape and when hardened can be a structural material. Portland cement can be used in mortars also (sand and water only) for screeds, plasters and in grouts.(17)

3.3.1 Portland cement composition

Clinker: Main constitute of Portland cement, which consist of Alite phase, Belite phase, Aluminate phase and ferrite phase.

Alite phase = C₃S = 3CaO.SiO₂

Alite constitutes approximately 55 to 60% of the clinker phase in Portland cement which is the major compound; it reacts with water and early in the hydration process release a significant amount of heat.(17)

Belite phase = C₂S = 2CaO.SiO₂

Belite constitutes about 20 to 25% of the clinker phase cements and with water shows much slower reaction compared to alite. The heat released is 25% of heat released in C₃S reaction.

Aluminate phase = $C_3A = 3CaO \cdot Al_2O_3$

Aluminate constitutes nearly 4-12% of clinker and from an engineering viewpoint presence of aluminates unfavorable since it leads to durability problems such as sulphate attack, C_3A act as flux to decrease energy requirements. It has rapid reaction with water and by adding gypsum, reaction can be controlled.(17)

Ferrite phase = $C_4AF = 4CaO \cdot Al_2O_3 \cdot Fe_2O_3$

This phase constitutes 5 to 10% of clinker composition, Iron like C_3A but not as reactive.

Ferrite similar to aluminate acts as fluxes to reduce energy requirements and since both hydration products make cement more vulnerable to durability problems, they are undesirable. Portland cements standards are mentioned in appendix A.(17)

Cement, water reaction:

$C_3S + Water$ Calcium Silicate Hydrate (C-S-H)

→ (Contributing to the strength of cement)

$C_2S + Water$ Calcium Hydroxide (CH)

(Cause durability problem with elapse of time)

Reactant Products:

Calcium Silicate Hydrate (C-S-H):

Approximate Formula: $C_3S_2H_3$

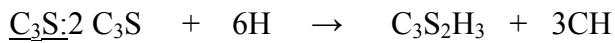
C-S-H is known as Tobermorite gel and has strong shape like Xonolite and main cementitious compound.

Exact formula varies depending upon composition, age, hydration temperature, presence of other materials like fly ash, slag, etc.(17)

Calcium Hydroxide (CH):

Platy like material which transition zone has a high CH content thus very porous.

Hydration of the Calcium silicates:



3.4 Oil well cement properties and categories

In petroleum industry, oil well cements are selected according to the API (American Petroleum Institute) specifications. Because the conditions to which Portland cement is exposed in wells can vary basically from those experienced in construction applications. API provides eight classes of oil well cements which are designated from class A through H. These eight classes are arranged based on depths that they are placed and the pressures and temperatures to which they are exposed. API classes A, B and C corresponds to ASTM types I, II and III; ASTM types IV and V have no corresponding API classes.(16)

3.4.1 Characteristics and Manufacturing process of oil well cements

One of the main characteristics of the oil well cement is that it is resistant to high pressure and also the high temperature. In certain fields, oil wells are subjected to pressure of 20,000 psi and 500 °F. The raw materials which are necessary for the production of oil well cement consist of limestone, iron ore and coke.(16)

3.4.2 Oil well cement grades and types

HSR (High Sulfate Resistant), MSR (Moderate Sulfate Resistant) and O (Ordinary type) are the three grades of oil well cements, which among these the O, Ordinary type is most commonly used.(16)

Class A:

Applicable for use from surface to a depth of 6,000 ft (1830 m) and special properties are not required. It is available only in ordinary type (O). (Similar to ASTM C150, type I).

Class B:

Applicable for use from surface to a depth of 6,000 ft (1830 m) when conditions require moderate to high sulfate resistance. Both moderate and high sulfate resistance types are available. (Similar to ASTM C150, type II).

Class C:

Applicable for use from surface to a depth of 6,000 ft (1830 m) when high early strength conditions are required. Ordinary type and moderate and high sulfate resistant types are available. High early strength and rapid hardening are characteristics of class C which allows to be used at higher water levels compared to G, H classes. Class C cement is finer when compared to other classes of cement and this class of cement has surface area of about 400- 500 m²/kg.

Class D:

Applicable for use from 6,000 to 10,000ft (1830 m to 3050 m) and also can be used at moderately high temperatures and pressures. Class D cement is available in both HSR and MSR grades and this type of cement has good pumpability.

Class E:

Applicable for use from 10,000 to 14,000 ft (3050 m to 4270m) depth under conditions of high temperatures and pressures. In both moderate and high sulfate-resistance types are available. A retarder must be added in the plant by the cement manufacturer to adjust its thickening time.

Class F:

Applicable for use from 10,000 to 16,000 ft (3050 m to 4880 m) depth under conditions of extremely high temperatures and pressures. Both moderate and high sulfate-resistant types are available. A retarder is added in the plant by the cement manufacturer to adjust its thickening time.

Class G:

Applicable for use as a basic cement from surface to a depth of 8,000 ft (2438 m) as manufactured. It can be used at a wide range of depths and temperatures with accelerators and retarders. It is specified that no additive except calcium sulfate or water, or both, shall be interground or blended with the clinker during the manufacture of class G cement. Class G is available in HSR and MSR grades and compatible with most of additives.

Class H:

Applicable for use as a basic cement from surface to depth of 8,000 ft (2438 m) as manufactured. This cement can be used with accelerators and retarders at a wide range of depths and temperatures. It is specified that no addition except calcium sulfate or water, or both, shall be interground or blended with the clinker during the manufacture of class H cement. Only in moderate sulfate resistant type is available. This type of cement Identical to class G but intended for higher density slurries. Typical composition and properties of API classes of Portland cement are indicated in table 3.1. Other application and types of oil well cement are given in appendix B.(16)

Table 3.1 Typical composition of API classes of Portland cement (16)

API Classes	Compounds (Percentage)				Fineness (surface area) (sq cm/g)
	C ₃ S	C ₂ S	C ₃ A	C ₄ AF	
A	53	24	8	8	1,600 to 1,800
B	47	32	5	12	1,600 to 1,800
C	58	16	8	8	1,800 to 2,200
D&E	26	54	2	12	1,200 to 1,500
G&H	50	30	5	12	1,600 to 1,800

3.5 Cement-CO₂-brine interaction in wellbore environment

Injecting carbon dioxide into the geological formation affects the brine chemistry and increase the system chemical reactivity. Understanding of carbon dioxide interaction with cement and formation water has huge impact on the successes of CO₂ storage. Injected CO₂ goes upward with favorable vertical permeability and with buoyancy effects, after few years of injection CO₂ gathers under the overlying cap rock and then dissolve in formation water of cap rock, move upward vertically into cap rock. The cap rock formation water is acidized when CO₂ is dissolved in it.

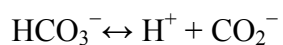
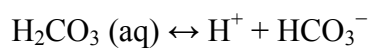
Another route of carbon dioxide migration is through well cement. Interaction of carbon dioxide and well cement has attracted interest since its implication in CO₂ storage. Migration of CO₂ through cement is a slow process and result in narrow carbonation zones over a period of 30 years. Actually, from reservoir into the cement there is no flow nevertheless, diffusion permits some CO₂ (aqueous form) to penetrate through cement. Carbonation of cement in the presence of CO₂ is well documented in literature. There is a discussion regarding whether or not the cement sheath (cement sheath is the cement which meet long term requirements imposed by the operational regime of the well) carbonation in wells are detrimental for effective zonal isolation. The primary purpose of cementing job is to provide effective zonal isolation for the life of the well therefore oil and gas can be produced economically and safely. When cement is exposed to CO₂ and water mixture, chemical reactions occur and mechanical properties degrade. Rate of carbonation depends on some factors such as moisture content, cement type, porosity, permeability, temperature and CO₂ partial pressure.(11)

3.6 Solubility of carbon dioxide in water

Carbon dioxide is soluble in water, in which there is an interconversion between carbon dioxide and carbonic acid spontaneously. For carbon dioxide solubility in water, a chart has been provided as a function of pressure and temperature which allows to a more precise determination of solubility of CO₂ in water and is given in Fig 3.2. Temperature and pressure affect the solubility of CO₂ in water. When temperature increases, the solubility of CO₂ decreases. Increase in temperature results

in an increase in kinetic energy. The higher kinetic energy causes more motion in molecules which break intermolecular bonds and escape from solution. The solubility of CO₂ in water is directly proportional to the pressure. If the pressure is increased, the CO₂ molecules are forced into the solution since this will best relieve the pressure that has been applied.(18)

The dissolved CO₂ in water follows reactions shown below:



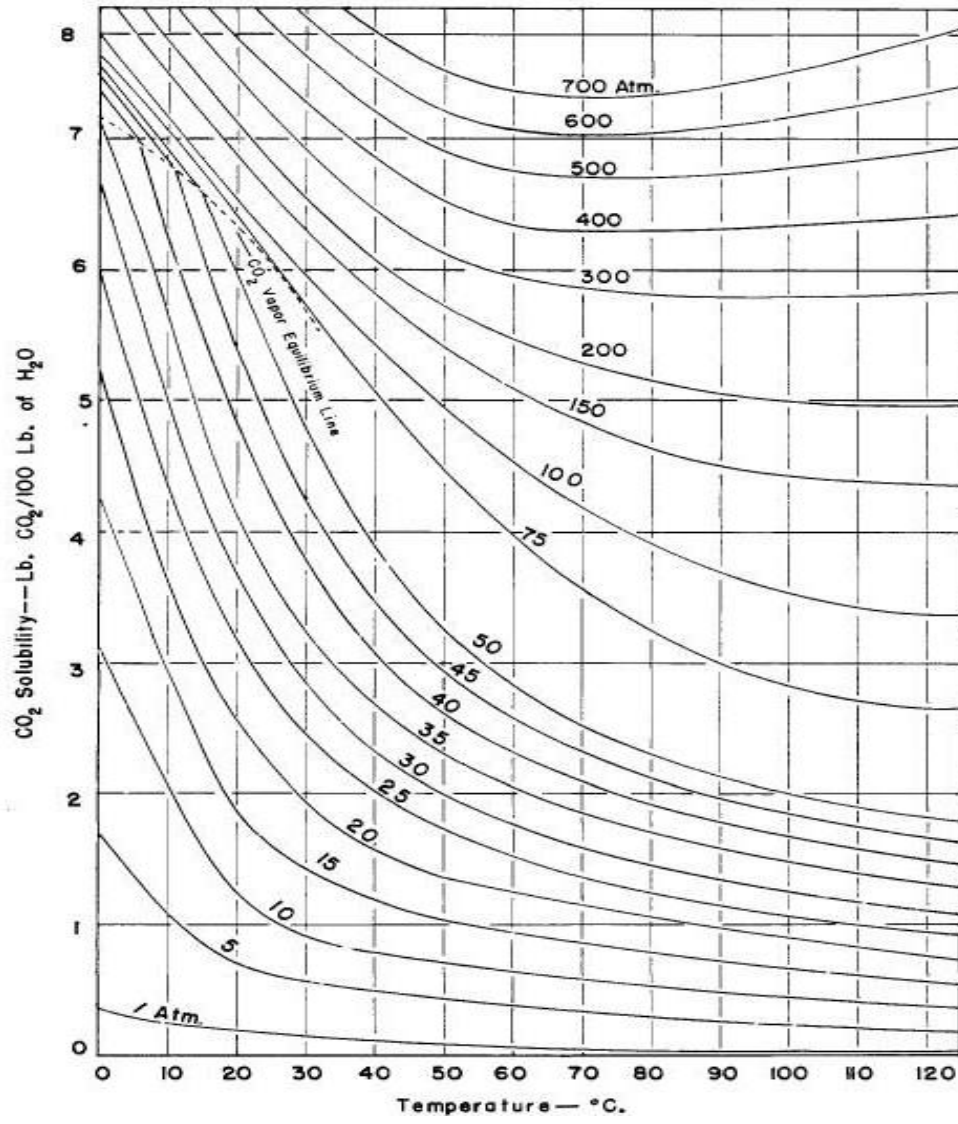


Fig 3.2 Solubility of carbon dioxide in water (temperature, pressure effects) (18)

3.7 Diffusion of CO₂ through cement

Diffusion of CO₂ through cement is a slow process and can lead to relatively narrow carbonation zones (~ 1 cm) over periods as long as 30 years. An alternative leakage scenario consists of flow of CO₂ through cement in production wells which is likely to be significantly more rapid than diffusion. However, CO₂ diffusion through cement is a function of the relative capillary properties of the cement, the interface zone (where CO₂-rock interaction occurs), and any pressure gradient imposed on the system.

The contrast in capillary properties between the cement and the formation rock containing CO₂ influences the extent of CO₂ penetration in the cement. Within the reservoir, cement will be in contact with rock having strongly contrasting capillary properties. Because the interface between cement and formation is vertical for non-deviated well, there is no hydraulic pressure gradient across the interface and CO₂ flow can only be driven by capillary forces. As a result, there is essentially no flow from the reservoir into the cement. However diffusion allows some CO₂ dissolved in water to penetrate the cement.(19)

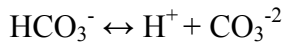
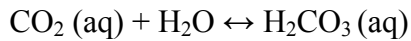
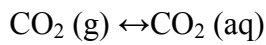
3.8 Chemical reactions due to Cement-CO₂-brine interaction

Three different reactions occur due to interactions of cement-brine-CO₂. First reaction is between CO₂ and brine and CO₂ dissolve in aqueous phase, then second reaction happens when carbonic acid comes to contact with hydrated cement, and finally the third reaction take place when the liquid water containing dissolved CO₂ surround the cement matrix.

First step: Carbonic acid formation

When there is a contact between CO₂ and water, carbonic acid (H₂CO₃) forms which means CO₂ dissolves in water.(10)

CO₂ dissociation



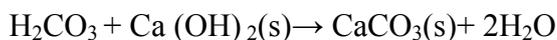
First step decreases the local pH, which also depends on partial pressure of CO₂, temperature and the ions present in water.(10)

Second step: Portlandite carbonation or cement hydrates

Calcium hydroxide Ca(OH)₂, the cementitious compound which is platy like material and responsible for low strength and non-durable performance of cement and Calcium Silicate Hydrate (Ca_{3,4}-Si₂-H₈), which is the main cementitious compound known as Tobermorite gel and responsible for the strength of cement.

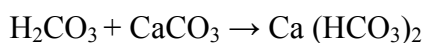
Cement dissolution

During cement dissolution process, first Ca(OH)₂ will be dissolved then CaCO₃ will be precipitated which improves the structural performance and also increase hardness and strength of cement and decreases the porosity and permeability of the cement matrix which reduce CO₂ diffusion.(10)



Third step: Calcium Carbonate Dissolution

This reaction takes place only when cement is surrounded completely with liquid water, containing dissolved CO₂. It is a long term phenomenon. Due to exposure to carbonic acid, calcium carbonate is subject to degradation.



The effects of this reaction is the loss of mechanical integrity, increase in porosity, permeability and in extreme cases leading to inefficient loss of zonal isolation which will occur over a long term. There are approaches, which help to reduce the detrimental impacts of carbonations:

- Decrease permeability, porosity by decreasing Ca(OH)_2 amount in cement.
- Reduce the cement amount by introducing filler.
- Altering the C-S-H composition to CO_2 resistive one as well as reduce the Ca(OH)_2 by adding supplementary cementitious materials such as fly ash, silica fume and etc.(10)

3.9 Basalt

The effectiveness of CO_2 storage depends on the reservoir stability, retention time and the reduced risk of leakage. One way to enhance the long-term stability of CO_2 is through the formation of carbonate minerals. The degree to which mineral storage is significant and the rate at which mineralization occurs depend on the rock type and also injection methods. Mineral carbonation of CO_2 could be enhanced by injection into silicate rocks rich in divalent metal cations like basalts. Basalt is a most common volcanic rock with grey to black color. It is silica rich and contains cations like iron, magnesium and calcium and form carbonate minerals when combine with CO_2 .

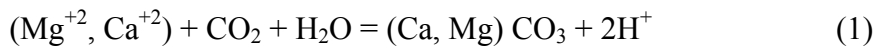
3.9.1 CO_2 - water-basalt interaction

For in-situ mineralization of CO_2 , basalt is considered as a promising reactant. Because this type of rock has high accumulation of calcium and magnesium silicate minerals. Dissolution of CO_2 in groundwater is slow which restricts the mineral precipitation and dissolution reactions. Water-basalt interaction at low concentrations of CO_2 have demonstrated clays, quartz, zeolites and calcite to be secondary minerals which are dominant while SiO_2 , Mg, Fe^{+2} and Ca carbonates are dominant at elevated CO_2 concentration. The significance of presence of basalt powder in oil well cement slurries is that they improve the fracture toughness of oil well cement slurries. Basalts have high tensile strength, alkali resistance, excellent resistance to

high temperature, resistant to acids and aggressive chemicals, completely inert with no environmental risks and available at low cost. (15)

3.9.2 In-situ mineral carbonation in basaltic rocks

Mineral carbonation requires divalent metallic cations, like Fe^{+2} , Ca^{+2} and Mg^{+2} for the carbonation process. When CO_2 reacts with Fe, Ca and Mg oxides, the corresponding carbonate is formed and heat is released. These oxides are prevalent in silicate minerals. Given the concentration of the oxides and their reactivity, focus on in-situ mineral carbonation has been on rocks rich in olivine, serpentine, pyroxene, plagioclase feldspar and basaltic glass. Crystalline basalt is rich in plagioclase feldspar, pyroxene and olivine and basalt, glassy and crystalline, contains 7-10 wt% Ca, 5-6 wt% Mg, and 7-13 wt% Fe. After injection of CO_2 in deep aquifers in basaltic rocks following exothermic chemical reactions are taking place:



According to the above reaction the divalent metallic cations in basalt react with CO_2 to precipitates carbonate minerals. For each mole of carbonate mineral precipitated, 2 moles of H^+ produced. The reaction (1) will not proceed to the right unless the H^+ ions are neutralized. Neutralization of H^+ will take place by reaction with the primary mineral phases in the basaltic host rock, as simplified in reaction (2) and (3).

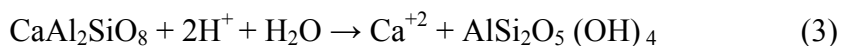
Common minerals in basalt are plagioclase, olivine, pyroxene, plagioclase feldspars. Forsterite (Mg_2SiO_4) composed of magnesium, oxygen and silicon is the magnesium rich end-member of the olivine solid series.

Forsterite,



Ca-plagioclase is a solid solution series and known as the plagioclase feldspar series.

Ca-plagioclase



Carbonate minerals precipitation depends on the pH. (15) Basalt minerals dissolution and the release of divalent cations contribute the pH of solution to increase until the precipitation starts. Since the calcite precipitation in reaction 1 is fast, the mineral carbonation extent is settled by dissolution kinetics of the reactions given as (2) and (3).

CHAPTER 4

STATEMENT OF THE PROBLEM

Carbon capture and storage for thousands of years in underground formations is one of the ways to reduce the amount of CO₂ emissions in the atmosphere. Underground CO₂ storage may have some effect on wellbore integrity and wellbore cement has been identified as the risk contributing to leakage of CO₂ from geologic carbon storage. The purpose of this thesis work is to investigate the chemical reactions that occurs between the CO₂ saturated brine and cement + additive mix and as additive basalt was added to cement mix.

The cement mix to be prepared by adding basalt in 0,10,20,30 cement basalt ratio in 4 cement plugs will be tested for physical properties and change in these properties to be studied on similar cement plugs subjected to CO₂-brine saturated under 1100 psi pressure and 65°C temperature. The change of cement plug properties after 3 months duration is to be tested. SEM photographs will visually show alteration in microscopic scale.

CHAPTER 5

EXPERIMENTAL SET UP AND PROCEDURE

The experiment is conducted under temperature of 65 °C and a pressure of 1100 psi. This is the situation where CO₂ is in saturated state. Before the experiment started, the temperature of the oven was raised to a temperature of 65 °C. The four cement plugs in core holders prepared and situated inside the oven, and then CO₂ saturated brine was sent to the top of cement plug at the same time. The experiment carried out for 90 days at constant pressure and temperature.

5.1 Materials used in experiment

Four cement plugs provided by TPAO for the experiment and the materials that used in these 4 samples consists of class G cement + basalt + water + additive (CFR).

The Class G cements provided by TPAO from Izmit, Nuh Cimento factory or which the chemical compositions are as indicated in table 5.1.

Table 5.1 Chemical composition of class G cement

Type	Chemical composition (weight percent)							
	SiO ₂	Al ₂ O ₃	Fe ₂ O ₃	MgO	CaO	K ₂ O	SO ₃	LOI
Class G Cement	22.43	4.76	4.10	1.14	64.77	0.08	1.67	0.54

Table 5.2 Chemical properties of class G cement (16)

Type	Compound (weight percent)			
	C ₃ S (3CaO.SiO ₂)	C ₂ S (2CaO.SiO ₂)	C ₃ A (3CaO.Al ₂ O ₃)	C ₄ AF (4CaO.Al ₂ O ₃ .Fe ₂ O ₃)
Class G Cement	50	30	5	12

Table 5.3 Physical properties of class G cement (16)

Type	Specific Gravity (average)	Absolute Volume (gal/lb)	Bulk Density (lb/ft ³)	Fineness (Surface area) (sq cm/g)
Class G Cement	3.15	0.0382	94	1600 to 1800

The other material that used for the samples as additive is basalt, for which the XRD analysis provided by Geology Engineering department of METU. The sample was from North of Kütahya, Kaynarga Village.

The chemical composition of basalt sample used is given in table 5.4:

Table 5.4 Chemical compositions of basalt used in experiment

Type	Chemical composition (weight percent)											
	SiO ₂	Al ₂ O ₃	Fe ₂ O ₃	MgO	CaO	Na ₂ O	K ₂ O	TiO ₂	P ₂ O ₅	MnO	Cr ₂ O ₃	LOI
Basalt	57.23	16.60	6.43	2.45	5.44	4.56	2.40	1.20	0.39	0.13	0.03	3.14

As the aqueous phase synthetic brine was prepared with composition given in below and the chemical analysis for cations was determined by ICPOES analyzer (inductively coupled plasma optical emission spectrometer) and the results are also given in table 5.5. The analysis was performed at METU central laboratory.

Table 5.5 Synthetic water analysis

Composition	mg/L
Na	551.3±8.5
Ca	24.2±0.1
Mg	43.9±0.1
Fe	0.02
K	2.40±0.03
S	6.78±0.10

For the above composition and also for the 1 L formation water preparation, 375.6 mg of $\text{MgCl}_2 \times 6\text{H}_2\text{O}$, 333 mg of CaCl_2 , 36.8 mg of $\text{MgSO}_4 \times 7\text{H}_2\text{O}$, 1.83 mg of $\text{FeCl}_3 \times 6\text{H}_2\text{O}$, 688 mg of NaCl and 1355 g of NaHCO_3 are added.

5.2 Cement slurry preparation

Four cement slurry samples were prepared with different basalt content, class G well cement with constant water-cement ratio of 0.44, CFR (cement friction reducer) additive. 600 g cement used for four samples with different basalt content. Sample # 1 mixtures consist of 600 gram cement, no basalt content (0% of cement weight), 264 g (44% of cement weight) water and no CFR additive (0% of cement weight). Sample # 2 mixture consist of 600 gram cement, 60 g basalt (10% of cement weight), 264 g (44% of cement weight) water and 1.5 g (0.25% of cement weight) CFR additive. Samples # 3 mixture consist of 600 gram cement, 120 g basalt (20% of cement weight), 264 g (44% of cement weight) water and 3 g (0.5% of cement weight) CFR additive. Sample # 4 mixture consist of 600 gram cement, 180 g basalt (30% of cement weight), 264 g (44% of cement weight) water and 3 g (0.5% of cement weight) CFR additive. Basalt weight % in whole mixture (cement +water +CRF) in sample # 1 is 0% in sample # 2, 6% in sample # 3, 9% and in sample # 4, 13% .Samples were mixed as given API specification recommended practice 10A/ISO 10426-1 and the compositions of four samples are shown in table 5.6.Preparation of cement plugs according to API recommended procedure and apparatus are given in Appendix C.

Table 5.6 Cement slurry compositions

Sample No	Class G cement (g)	Basalt (g)	Water (g)	CFR-3(cement friction reducer) (g)
1	600	0	264	0
2	600	60	264	1.5
3	600	120	264	3.0
4	600	180	264	3.0

A quality control test was carried out on class G cement to check the quality and capability of class G cement. Test results are given in table 5.7

Table 5.7 Class G cement quality control results

Free Water % 44 (Max 5.9, W %)	Thickening Time (Min)		Compressive Strength (Psi)	
	15-30 Max Bc (Max 30)	100 Bc duration (between 90-120)	8 hours in 30 °C (Min 300 psi)	8 hours in 60 °C (Min 1500 psi)
5.9	18	120	535	1967

Bc = Burden of Consistency, The pumpability or consistency of a slurry, measured in Bearden units of consistency (Bc), a dimensionless quantity with no direct conversion factor to more common units of viscosity.

Basalt was grounded into finer particles in three stages. The first stage, stone crusher used to grind basalt rock into smaller particle. In second stage, the small particle of basalt grinded again to make the particles smaller and in the third stage, ball mill was used to grind the basalt particle into extremely fine powder and then a sieve with mesh size # 200 (75 µm) used to obtain the basalt powder in 75 µm diameter.

After the material preparation was completed, the materials were mixed with amounts given in table 5.6. The cement slurry samples poured in cylinder holders with dimension of 2.634 × 2.307 inch. Then, the holders placed in the ultrasonic cement analyzer apparatus to determine the compressive strength at the specific pressure and temperature. After 24 hours the consistency and compressive strength

of four samples under 60 °C temperature and 1000 psi pressure was measured. The compressive strength graphs of all 4 samples are given in figures 5.1 to 5.4. The final compressive strength of 4 sore samples after 24 hours at 60 °C temperature and 1000 psi pressure are given in table 5.8. As table shows the final compressive strength of cement plugs increased as basalt content increased.

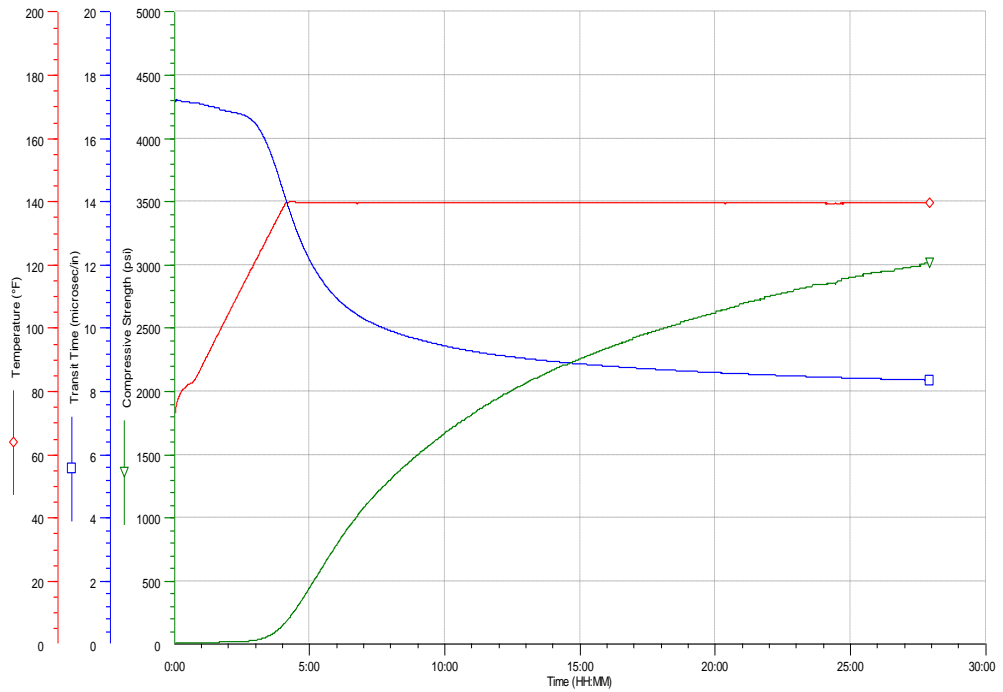


Fig 5.1 Compressive strength of sample # 1

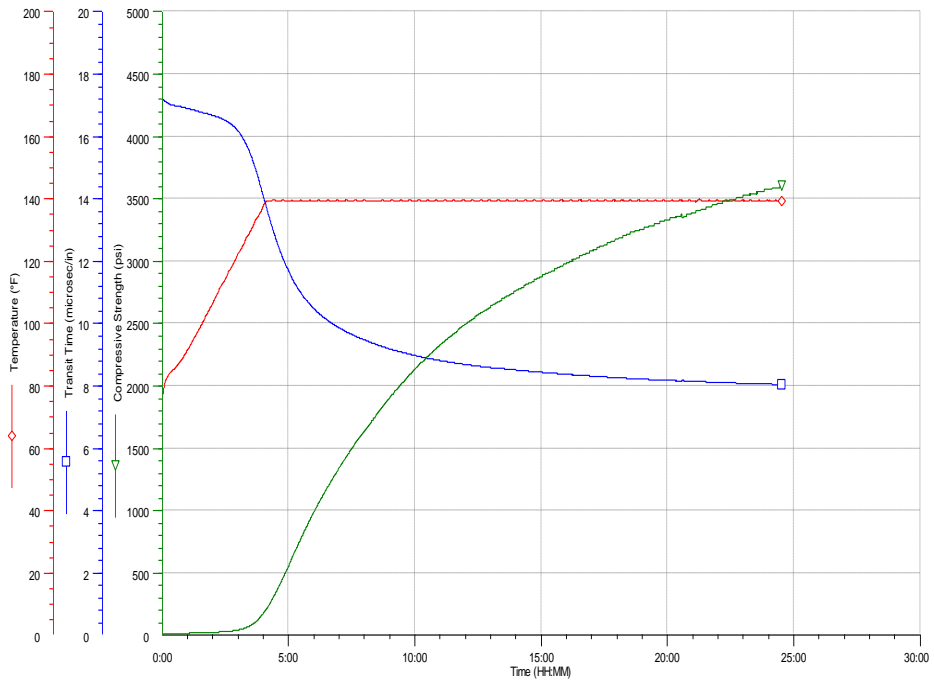


Fig 5.2 Compressive strength of sample # 2

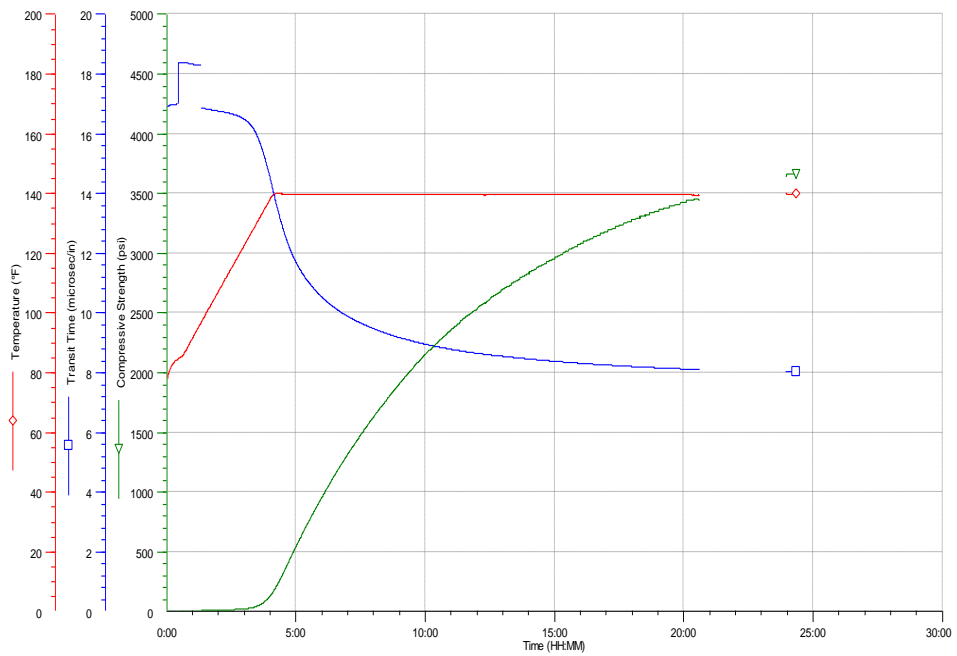


Fig 5.3 Compressive strength of sample # 3

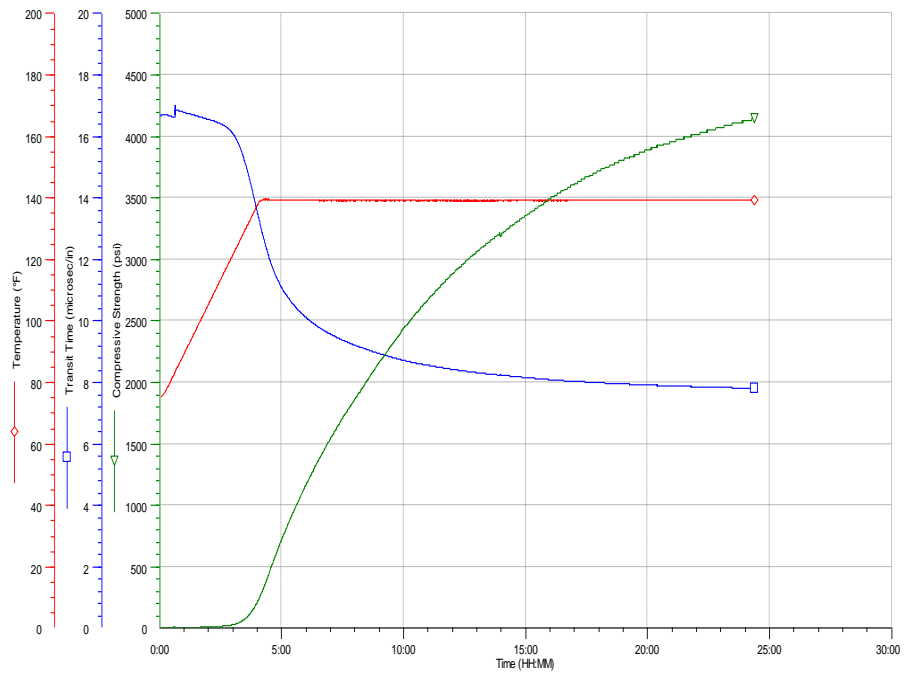


Fig 5.4 Compressive strength of sample # 4

Table 5.8 Compressive strength of 4 cement plugs

Samples	8 hr strength (Psi)	12 hr strength (Psi)	24 hr strength (Final Strength) (Psi)
Sample # 1 (cement+0%basalt)	1302	1945	3008
Sample # 2 (cement+6%basalt)	1633	2484	3598
Sample # 3 (cement+9%basalt)	1630	2528	3653
Sample # 4 (cement+13%basalt)	1864	2874	4138

5.3 Experimental set up

Cement plugs were prepared with 2.634×2.307 inch dimension and 1×2 inch dimension plugs were taken to fit the specific core holders which were used in experiment. The cement plugs # 2 and 3 were coated with teflon and placed in core holders while plugs # 1 and 4 were not coated since had same diameter with the inner diameter of the core holders. The experiment is conducted under the reservoir condition of a temperature of $65\text{ }^{\circ}\text{C}$ and a pressure around 1100 psi. This is the situation where CO_2 is in saturated state. Before the experiment started, the temperature of the oven was raised to a temperature of $65\text{ }^{\circ}\text{C}$. The four cement plugs in core holders situated inside the oven, and then CO_2 saturated brine sent to the top of the cement plugs at the same time. The experiment carried out for 90 days at constant pressure and temperature.

The set-up of experiment consist of an oven which keep the temperature constant at $65\text{ }^{\circ}\text{C}$, The mixing cylinder used for keeping CO_2 -water mixture, an ISCO pump for pumping water into the mixing cylinder, CO_2 cylinder, which contains $\text{CO}_2(\text{g})$. Thermocouples which connected from one side to data logger and the other side to the oven to record the temperature of oven, pressure transducer used to measure and record the pressure of four samples, Data logger which record the pressure and temperature and connected to PC, PC used to show everyday recordings. The set up for the experiment is shown in Figure 5.5.

The experimental equipment technical specifications are given in table 5.9 as observed from Figure 5.5. The four core holders and also the mixing cylinder, all are made of stainless steel and these holders are resistant to corrosion. For four cores the synthetic water analysis and the SEM analysis were carried out to observe any alteration due to CO_2 -saturated brine on cement basalt mix.

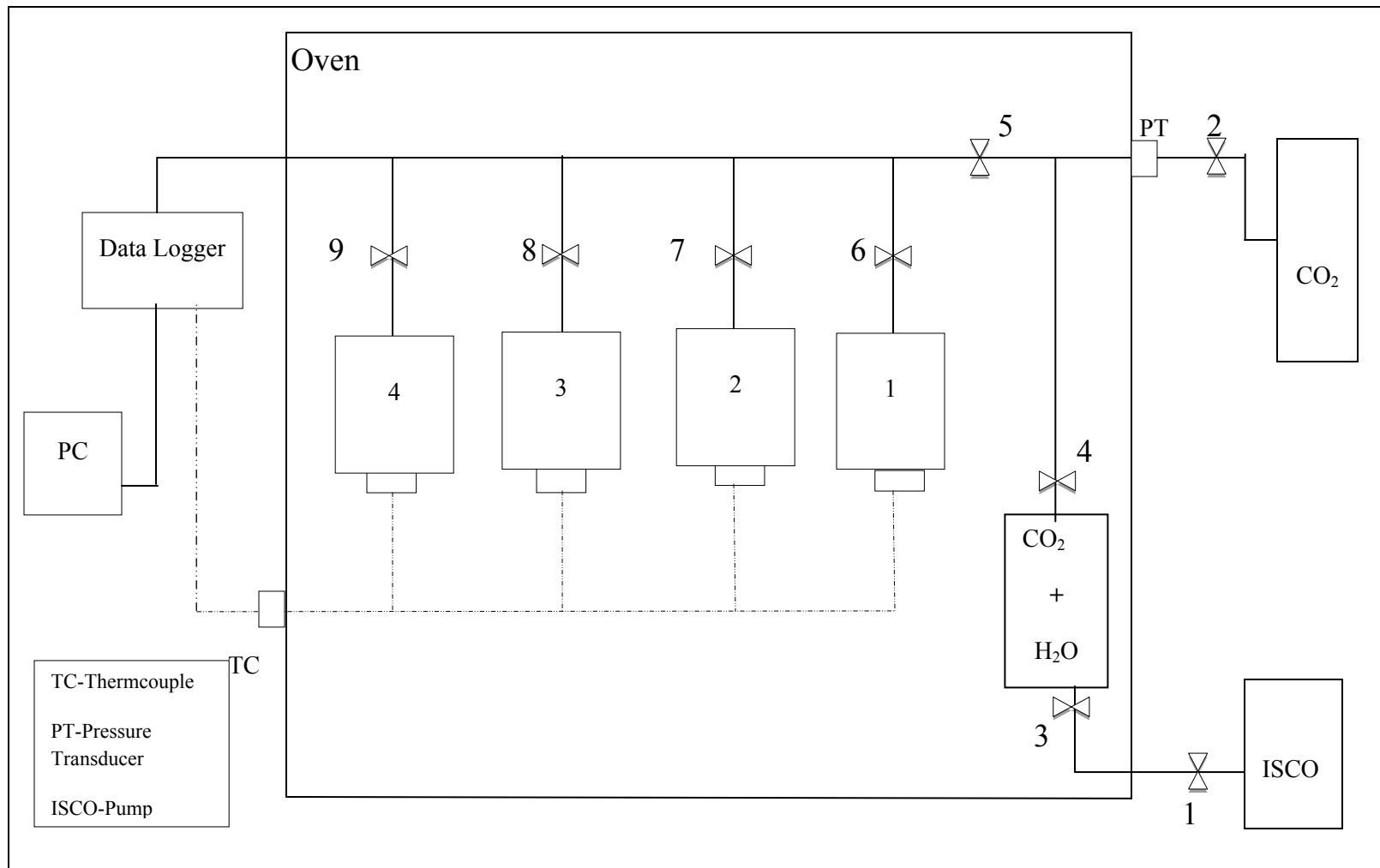


Fig 5.5 The schematic diagram of the experimental set-up

Table 5.9 Experimental apparatus and technical specification

Experimental apparatus	Technical specification
ISCO 500D Pump	Capacity of Cylinder: 266.38 ml Range of Pressure: 10 psi-3750 psia Depressurization or refill rate: 1 μ l/min-204 ml/min at any pressure 0-3750
Mixing Cylinder	High Pressure Steel, Height (21.5) cm, Diameter (3) cm Volume (151.89) cm^3
Thermocouple (PT-100)	-20 $^{\circ}\text{C}$ - +150 $^{\circ}\text{C}$
Pressure Transducer	0-3000 psia 4-20 mA
CO ₂ Cylinder	65.8 kg, 40 lt., 250 bar
Core Holders	High Pressure Steel, Height (5) cm, Diameter (2.54) cm Volume (25.32) cm^3
Elimko 680 Data Logger	Input types: Thermocouple, resistance Thermocouple, Voltage, Current Operating Temperature: -10 $^{\circ}\text{C}$ - +55 $^{\circ}\text{C}$ Memory: EEPROM max. 10^5 writing
Dispatch Oven	10-400 $^{\circ}\text{C}$

5.4 Experimental procedure

Before starting the experiment, the four core holders were pressurized up to 1000 psi by air and placed into the water bath to test for leakage. The parts of set up were assembled and the mixing cylinder and core holders vacuumed. 266.38 ml synthetic formation water was filled into the cylinder of ISCO pump. The experiment was carried out under 1100 psi pressure and 65 °C temperature. As Figure 5.5 exhibits, firstly CO₂ was conducted to the mixing cylinder by opening the valve # 3 and #4 at a pressure of 300 psia. Secondly, synthetic water formation from ISCO pump was sent to the mixing cylinder at a constant pressure of 1500 psia, then, in mixing cylinder, water and CO₂ was allowed to equilibrate for 4 hours and the pressure transducer recorded the pressure of mixing cylinder at around 1500 psi but since CO₂ is dissolving in synthetic water, the pressure started to decrease but after some hours leveled off at 1100 psi. After CO₂ completely dissolved in synthetic water, valves #4, #5 and #6 were opened and the core holder #1 is filled with the mixture and after the core holder #1 filled completely the valve #6 closed then Valves #4 and #5 and #7 were opened and allow the core holder #2 be filled with the mixture and after the core holder #2 filled completely the valve #7 closed, valves #4 and #5 and #8 were opened and allow the core holder #3 be filled with the mixture and after the core holder #3 filled completely the valve #8 closed, Valves #4 and #5 and #9 were opened and allow the core holder #4 to be filled with the mixture and after the core holder #4 filled completely the valve #9 was closed respectively. After sending the mixture to the four core holders, the valve # 1, 3, 4, 5, 6,7,8,9 were opened to pressurize the four holders in the same time, so the pressure of four core holders was raised to 1100 psi by pumping synthetic water form ISCO pump. The pressure of the system was recorded by pressure transducer which is connected to data logger and then the valves # 1, 2, 3, 4 were closed to allow recording the pressure of four core holders. The pressure and temperature of 4 core holders were recorded as illustrated in Figure 5.6 and all the temperatures and pressures were kept constant. The photos of set up and cement plugs are illustrated in Appendix D.

5.5 Amount of CO₂ used in experiment

Since the volume of cylinder calculated is 151.89 cm³ and CO₂ was sent to this mixing cylinder at a temperature of 65 °C and 300 psia (20.41 bar) partial pressure of CO₂ pressure, so the amount of CO₂ in brine can be calculated from

$$PV=ZnRT$$

$$n = \frac{PV}{zRT}$$

The critical temperature for carbon dioxide is 31.1°C, and the critical pressure is 73 atm. Reduced critical pressure and temperature are calculated as

$$P_r = \frac{P}{P_c} = \frac{20.41}{73} = 0.279$$

$$T_r = \frac{T}{T_c} = \frac{65+273}{31.1+273} = 1.111$$

At the condition of $P_r = 0.279$ and $T_r = 1.111$

$$z \approx 0.92$$

$$R = 8.314472 \text{ cm}^3 \text{ MPaK}^{-1} \text{ mol}$$

$$P = 300 \text{ psia} = 2.068 \text{ MPa}$$

$$T = 65 \text{ °C} = 338.15 \text{ °K}$$

$$n = \frac{151.89 \times 2.068}{338.15 \times 8.314472 \times 0.92} = 0.121 \text{ mole}$$

0.121 moles of CO₂ was mixed and dissolved in synthetic water which was in contact with each cement plug. Fig 5.6 represents the pressure and temperature recordings of the static experiment for last 5 days.

As figure 3.2 shows the solubility of carbon dioxide in 65 ° C temperature and 300 psi (20 bar) partial pressure of CO₂ is 1.4 lb CO₂ in 100 lb of H₂O. The 1.4 lb

solubility of CO₂ in 100 lb of H₂O correspondence to the 0.048 mole solubility of CO₂ in of 151 cm³ of H₂O. From the calculations, 0.121 moles of CO₂ is dissolved in synthetic water while the graph in figure 3.2 shows that in 65 °C temperature and 300 psi, 0.048 mole of CO₂ can be soluble in water, which indicate that all amount of CO₂ was not dissolved in water.

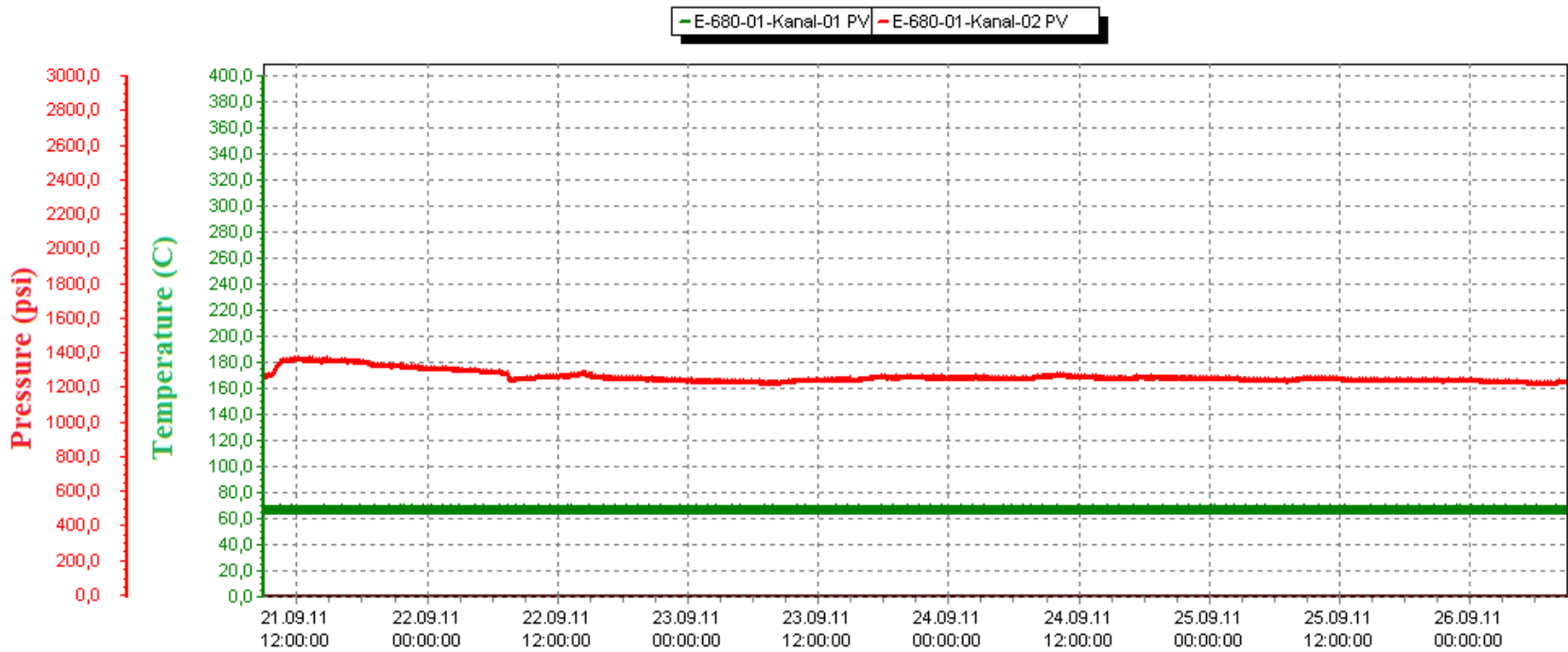


Fig 5.6 Pressure and temperature recordings of experiment (final 5 days)

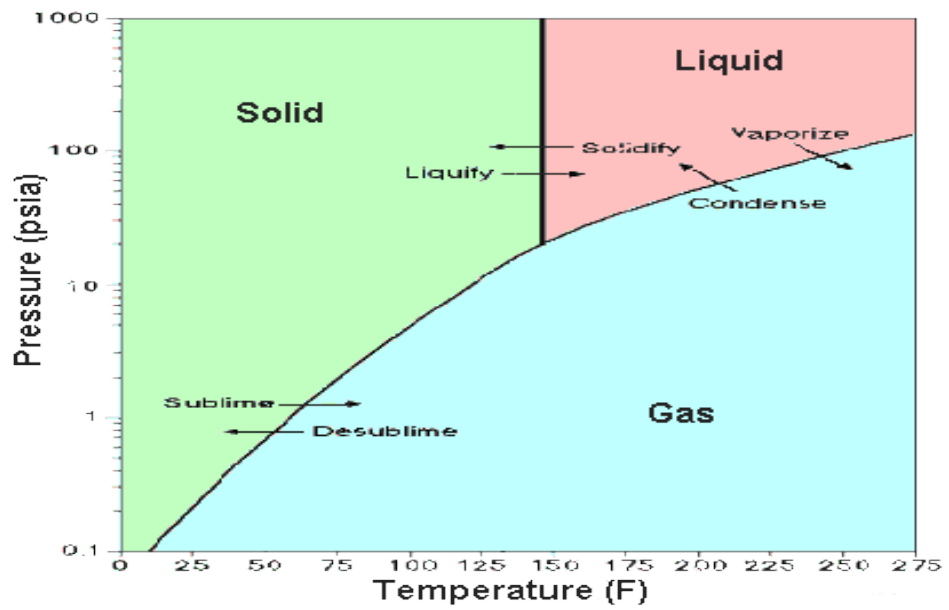
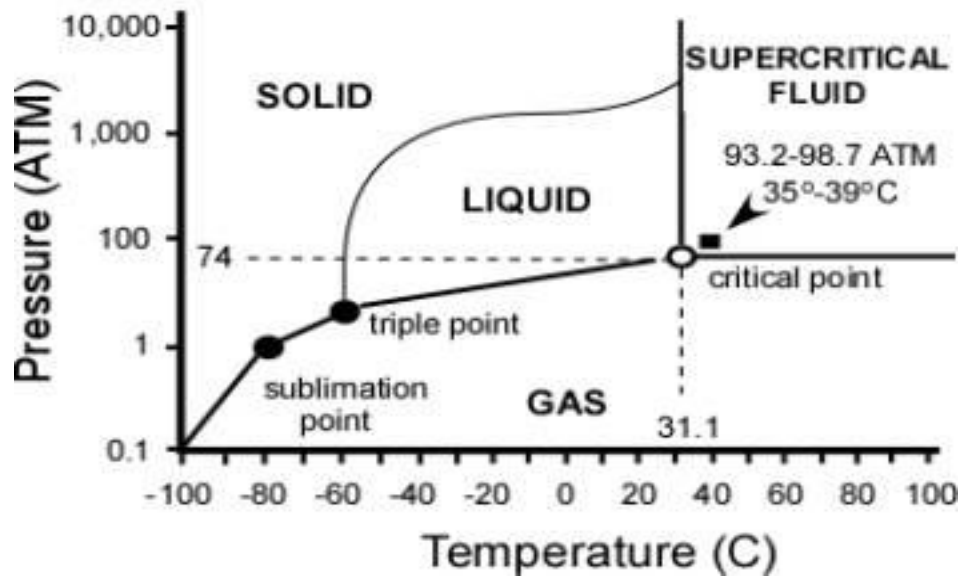


Fig 5.7 Carbon dioxide phase diagram (12)

CHAPTER 6

RESULTS AND DISSCUSION

This thesis work is carried out to investigate the possible chemical reactions between CO₂-water-cement interaction where cement had various concentrations of basalt as an additive and it affect the porosity, permeability and compressive strength of samples.

6.1 Synthetic formation water analysis results of four cement plugs

After the formation water prepared, has been mixed with CO₂ and sent to the core holders and the result of the CO₂ saturated brine after injection of 3 months of four samples is presented in table 6.1

Table 6.1 Synthetic formation water result

Compositions (mg/L)	Initial composition of water (mg/L)	CO ₂ water mixture (mg/L)	Final composition of water in contact with each cement plug after 90 days			
			1	2	3	4
Na	551.3±8.5	606±10	1491±6	5091±42	6135±103	6148±69
K	2.40±0.03	1.98±0.03	2993±126	5272±69	5515±105	4482±142
Mg	43.9±0.1	41.5±1.8	190±6	30.5±0.4	35.1±1.2	76.8±1.4
Ca	24.2±0.1	14.8±0.4	48.8±0.2	24.1±0.4	6.46±0.12	16±0.2
Fe	0.02	-	1.22±0.04	0.93±0.08	-	-
S	6.78±0.10	13.8±0.3	402±19	456±8	268±15	721±35

According to table 6.1 Na concentration in CO₂ treated water compared to initially prepared water had increased. The increase in Na concentration in CO₂ treated water is not expected and might be an experimental error, because there is no any reasonable explanation for its increase. The Na concentration of water samples obtained from core holders after 90 days shows an increase, so there must have been some dissolution of Na containing minerals from the cement plug. The concentration of Mg increased in sample # 1 from its concentration in CO₂ water mix which means Mg dissolved in water after 90 days while in sample # 2 and 3 Mg concentration decreased due to Basalt content .Basalt content in sample # 2 (6% basalt) and 3 (9% basalt) cause Mg concentration in water to decrease which means some amount of Mg precipitated. Mg concentration in water in sample # 4 (13% basalt) increased which was expected to decrease; there is no reasonable explanation for this. Ca concentration in sample #1 increased from its concentration in CO₂ water mix due to its dissolution in water. In sample # 2 (6% basalt)small amount of Ca precipitated while in sample # 3 (9%) by increasing basalt amount only 6.46 mg/L of Ca dissolved in formation water and the remaining amount is precipitated.Ca dissolved more in water in sample # 4 rather than in sample # 3 which there is no reasonable explanation for this. The comparison graphs of the element concentration in CO₂-water mix and four cement plug are illustrated in appendix E.

6.2 Porosity, permeability measurements of cement plugs before CO₂-brine treatment

The porosity and permeability of four samples by the specific apparatus based on API Recommended Practice 40 were also measured and the results are presented in table 6.2 As table 6.2shows, sample# 1 which consists of neat cement and water without any additives has the highest porosity while the porosity in sample # 2 (with 6% basalt), decreased. This indicates that fine particle size of the basalt migrate through cement matrix pores and decrease the porosity. In sample# 3 and 4 also decreases can be seen in porosity due to 6% and 9% increases in basalt particles addition respectively. The permeability of four samples before CO₂ injection has been measured and the results are shown in table 6.2 which there is a decrease trend also in permeability from sample# 1 to 3 but in sample # 3 the permeability increased

which there is no any reasonable explanation. The permeability of sample# 4 is less than others because of basalt content which is 13%, the increased basalt content the less the permeability. The porosity, permeability measurement apparatus are given in appendix F.

Table 6.2 Porosity, permeability values of four cement plugs before CO₂ injection

Sample No	Sample diameter (mm)	Sample Length (mm)	Core Porosity (%)	Ka (mD)
1	23.41	46.70	30.65%	0.035
2	23.25	46.70	29.15%	0.010
3	23.35	47.80	27.31%	0.025
4	23.35	47.70	27.27%	0.009

6.3 Porosity, permeability measurements of cement plugs after CO₂-brine treatment

The porosity and permeability of four samples by the specific apparatus based on API Recommended Practice 40 has been measured after 90 days. The results are presented in table 6.3. In sample # 1 because of the sample broke while dismantling from core holder, permeability and porosity values were not determined. The porosity of sample # 2 before CO₂ treatment was 29% while decreased to 22.30 % after CO₂ treatment (table 6.3) which indicates the effect of basalt, cement, and CO₂ brine saturated interaction in decreasing the porosity. In sample # 3 and 4 also porosity decreased with respect to basalt content. The permeability of four samples after CO₂ injection has been measured and the results are shown in table 6.3 which there is a decrease trend also in permeability from sample # 1 to 4 due to the addition of basalt particles. In sample # 4, does not have precise result for permeability since

half of the cement plug broke. By comparison the permeability result of tables 6.2 and 6.3, the permeability of samples# 2 and 3 has been decreased because when CO₂ saturated brine interact with the cement plugs which consist of cement, basalt mix and as result of this reaction, minerals such as CaCO₃ and Mg, Fe (CO₃) participated and act like a carbonate barrier which prevented from diffusion of CO₂ saturated brine into the cement plugs.

Table 6.3 Porosity, permeability values of four cement plugs after CO₂ injection

Sample No	Sample dia (mm)	Sample Length (mm)	Core Porosity (%)	Ka (mD)
1	23.41	46.70	*	*
2	23.25	46.70	22.30%	0
3	23.35	47.80	18.70%	0
4	23.35	47.70	17.48%	*

*In sample # 1 and 4 because of the sample broke while dismantling from core holder permeability and porosity values were not determined.

The measurement of porosity and permeability tests were conducted on cement plugs which were drilled from the original cement plugs which had larger diameter to fit the Ultrasonic cement analyzer apparatus.

6.4 Compressive Strength analysis of cement plugs

AP-1000 VERSA-TESTER apparatus was used for measuring the compressive strength of samples. Compressive strength was measured by applying a vertical load on the surface area of each sample. The device recorded the amount of load applied to the sample until the sample breaks. The load amount divided by surface area of sample is the compressive strength of the sample. Schematic of the apparatus is presented in Appendix G.

The strength of 4 cement plugs has been measured before and also after the CO₂ saturated brine treatment and the results of the measurements are shown at table 6.4 and 6.5:

Two different methods were used to measure the compressive strength of cement plugs before and after experiments. The compressive strength of cement plugs were measured by the ultrasonic cement analyzer apparatus before the experiment. Cement plugs used in CO₂-brine saturated exposure experiments were drilled to a smaller diameter so the measurement of the compressive strength after the experiment was realized using the AP-1000 VERSA-TESTER apparatus

Table 6.4 Compressive strength of 4 samples before CO₂ saturated brine treatment (by Ultrasonic cement analyzer)

Sample #	Amount of load applied up to break time (lb)	Surface area of samples (in ²)	Compressive Strength (lb/in ²)
1	2140	0.785	2726
2	2920	0.785	3719
3	3710	0.785	4726
4	4050	0.785	5159

As table 6.4 shows the compressive strength of samples has been increased significantly by increasing the basalt amount in samples from 0% up to 13%.

**Table 6.5 Compressive strength of 4 cement plugs after CO₂ treatment
(AP-1000 VERSA-TESTER apparatus)**

Sample #	Amount of load applied up to break time (lb)	Surface area of samples (in ²)	Compressive Strength (lb/in ²)
1	-	-	-
2	6330	0.785	8063
3	8590	0.785	10942
4	-	-	-

As it is presented in table 6.5 sample # 1 and 4 do not have any values because sample # 1 was broken and compressive strength cannot be measured. Sample # 4 bended while applying the vertical load (Fig 6.1). Samples # 2 and 3 compressive strength has been increased significantly with regard to two samples before CO₂ treatment. Cement samples # 2 and 3 containing basalt ultimately show improved durability to acid attack and increased the strength of the cement. Since the acid attack in cement and basalt mix cause carbonation so the carbonated part shows more uniform microstructure containing CaCO₃ and Mg, Fe (CO₃).⁽⁹⁾ Photographs of cement plugs after experiment are given in appendix H.



Fig 6.1 Cement plug 4 while applying vertical load

6.5 SEM analysis

SEM analyses of the cement plugs were carried out to investigate any structural and mineralogical changes on the core surfaces. The samples taken for SEM analysis were surface part where CO₂-brine contact was present about 1 to 2 cm depth of cement plugs. From the photographs taken in SEM analysis for the 90 days experiment, it is seen that the near to surface particles are more loose than the inner part of the core, which shows the CO₂ diffusion into the core. Invaded zone (color change) can be observed in samples # 1,2,3 while in sample # 4 the invaded part was negligible because color change was not identified which means 13 % basalt content in sample# 4 make the sample more resistant to carbonic acid diffusion. The part of the sample where carbonic acid diffuse (invaded zone) is the carbonated zone and the part which there is no any diffusion is uncarbonated zone. As it is obvious from figure 6.2 the sample # 1 (neat cement without basalt additive) shows the formation of three distinct zones. First zone which has 1.5 mm length carbonic acid penetration is the porous zone where presumably Ca(OH)₂ is dissolved; the dissolution of Ca (OH)₂ increased the porosity of the sample. The second zone which has about 0.25 mm length is less porous zone and is the zone where CaCO₃ precipitated. The formation of CaCO₃ decreased the sample permeability and increased its compressive strength. The third zone which is beyond the second zone is unaltered zone, where the CO₂ saturated brine did not diffuse. In Figure 6.3 the first zone in sample # 2 has about 0.75 mm length carbonic acid penetration, the second zone has about 0.5 mm length. In Figure 6.4 the first zone in sample # 3 has about 0.5 mm length carbonic acid penetration, The second zone has about 1.25 mm length. The surface images of samples from side of the cement plug after CO₂ saturated brine treatment are presented in figure 6.2~6.4.

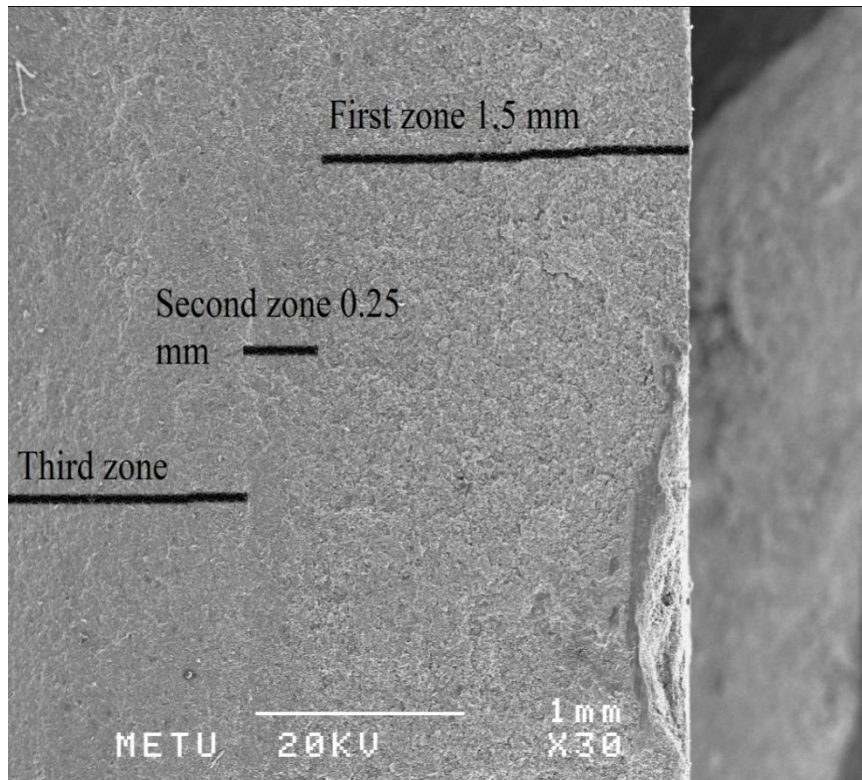


Fig 6.2 SEM surface image of cement plug 1 after 3 months CO₂ saturated brine treatment

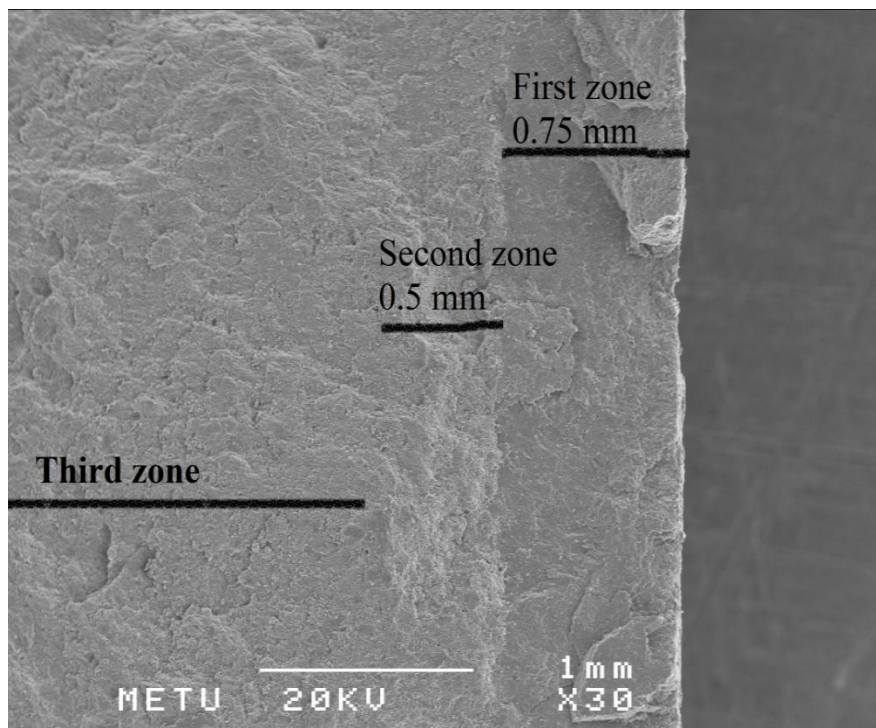


Fig 6.3 SEM surface image of cement plug 2 after 3 months CO₂ saturated brine treatment

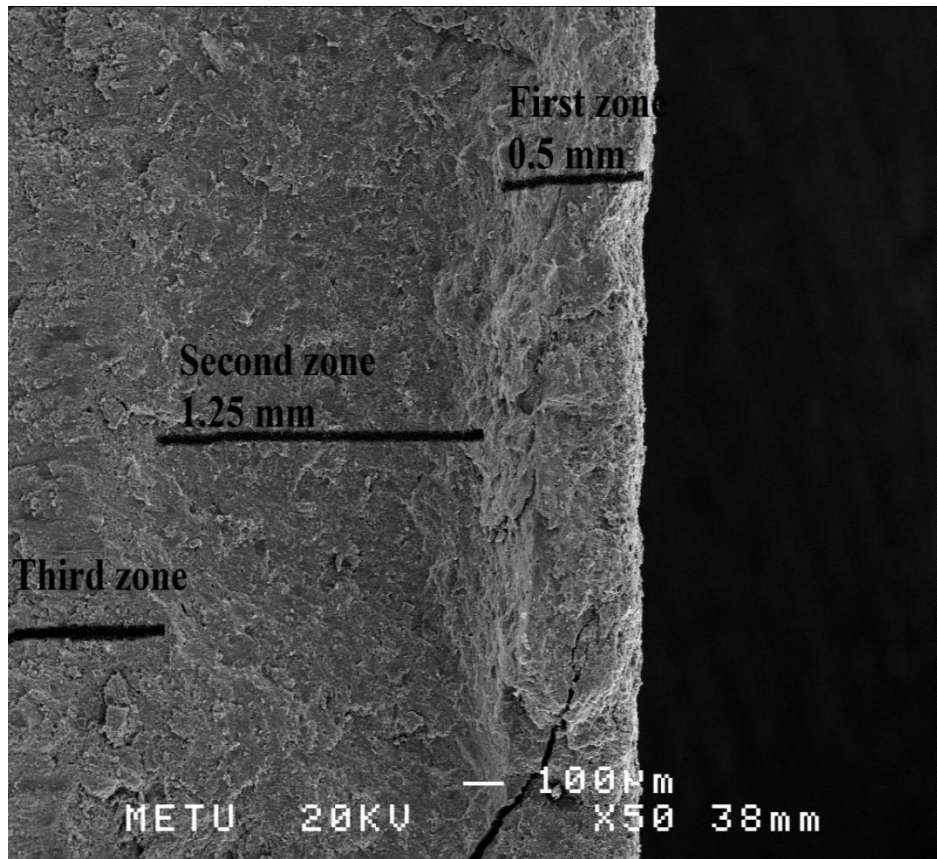


Fig 6.4 SEM surface image of cement plug 3 after 3 months CO₂ saturated brine treatment

SEM analysis was carried out for whole samples from near surface of samples where carbonic acid diffused and inner part of samples where no diffusion occurred, EDS (Energy dispersive spectrometry), analysis was obtained after 90 days experiment. Based on the result of the EDS in tables I.9~I.16 in appendix I, sample # 1 weight percent of Mg and Ca near to surface is less than the inner section of sample # 1, can be interpreted that some amount of Mg and Ca dissolved in carbonic acid. Si weight percent increase near to surface of sample # 1 compared to inner part which might be interpreted that Si precipitated after the reaction with carbonic acid. In sample # 2 weight percent of Mg and Ca near to surface is less than the inner section of sample # 2, which shows that some amount of Mg and Ca dissolved in carbonic acid. In sample # 3 weight percent of Mg and Ca near to surface is less than the inner section of sample # 3, can be interpreted that some amount of Mg and Ca dissolved in carbonic acid.

In sample # 4 weight percent of Mg near to surface is less than the inner section of sample # 4, can be interpreted that some amount of Mg dissolved in carbonic acid. Ca weight percent near to surface is higher than the inner section can be interpreted that some amount of Ca precipitated in carbonic acid. The photographs of near to surface and also inner section view of in depth SEM/EDS analysis for whole cement plugs before and after experiment are given in appendix I. The SEM/EDS analysis which were carried out from near to surface and also inner section of samples are not exactly from the same area section of the samples so the element concentrations could not be compared properly.

CHAPTER 7

CONCLUSION

Safe and effective geological storage of CO₂ requires the consideration of several factors. The effectiveness of CO₂ storage operation depends strongly on the retention time, reservoir stability and risk of leakage. In this thesis work the chemical alteration of oil well cements in CO₂ brine environment was investigated where 0,6,9 and 13 weight percent of cement, basalt fine particles were added to cement slurry. Conclusions are:

- Cement plugs compressive strength has been increased significantly with regard to basalt content of 0, 6, 9 and 13 weight percent. Cement plugs containing basalt ultimately show improved durability to acid attack and increased the strength of the cement. Since the acid attack in cement and basalt mix cause carbonation so the carbonated part shows more uniform microstructure containing CaCO₃ and Mg, Fe (CO₃).as stated by(9).
- It can be interpreted that three distinct zones were formed in cement plugs. First zone is the porous zone where Ca(OH)₂ is dissolved; the dissolution of Ca(OH)₂ increased the porosity of the sample. The second zone is less porous zone and is the zone where CaCO₃ precipitated. The formation of CaCO₃ is expected to decrease the permeability and increase cement plug compressive strength. The third zone is unaltered zone, where the CO₂ saturated brine did not diffuse through.

- Change in depth of penetration (movement of carbonation front) from cement plugs 1~4 indicate that increasing basalt amount create CO₂ resistance of cement to carbonic acid.
- Carbonation of cement blends (cement + basalt) improved structural performance in that it reduces porosity and permeability and increases the mechanical strength of the cement matrix.

REFERENCES

- (1). Research, International Public-Private Sponsored, "Global Energy Technology Strategy, www.osti.gov/energycitations/. Retrieved September 2011.
- (2). "IEAGHG. IEAGHG R&D Programme", International Energy Agency (IEA), (2010) www.ieaghg.org. Retrieved September 2011.
- (3). "The Global Status of CCS 2011 publication", (2009). Retrieved September 2011.
- (4). "CO₂ Storage Sites", (2006) www.CO2remove.com. Retrieved September 2011.
- (5). Onan. D, Halliburton Services, "Effects of Supercritical Carbon Dioxide on Well Cements" Society of Petroleum Engineers 12593, 1984.
- (6). V.Barlet-Gouedard, G.Rimmele, O.Porcherie, N.Quisel, J.Desroches, "A solution against well cement degradation under CO₂ geological storage environment", International journal of greenhouse gases control, 2009.
- (7). Barbara G. Kutchko, "Degradation of well cement by CO₂ under geologic sequestration conditions", Environmental science and Technology ,Vol. 41. 2007.
- (8). Barbara G. Kutchko, et al, "Rate of CO₂ attack on hydrated class H well cement under geologic sequestration conditions", Environmental Science and Technology, Vol. 42, 2008.
- (9). Barbara G. Kutchko, "CO₂ reaction with hydrated class H well cement under geologic sequestration conditions: Effects of flyash admixtures" Environmental science and Technology, Vol. 43, 2009.
- (10). Ashok Santra, B.R.Reddy, Feng. Liang, Rocky. Fitzgerald, Haliburton "Reaction of CO₂ with portland cement at downhole conditions and the role of pozzolanic supplements". Society of Petroleum Engineers 121103, 2009.

- (11).W.Carey and P.C.Lichtner, Los Alamos National Laboratory,"Computational studies of two-phase cement-CO₂-brine interaction in wellbore environments". Society of Petroleum Engineers 126666, 2009.
- (12). Nediljka Gaurina-Medimurec "The influence of CO₂ on well cement",Hrcak portal of scientific journals of Croatia,Vol.22, 2010.
- (13).Koji. Takase, Japan CCS Co.,Ltd, Yogesh Barhate, Hiroyuki Hashimoto,SPE,Halliburton and and Siddhartha F.Lunkad, Formerly Halliburton"Cement-sheat wellbore integrity for CO₂ injection and storage wells",Society of Petroleum Engineers 127422, 2010.
- (14). R.Felicetti, C.Meyer, S.Shimanovich"Basalt fiber reinforced oil well cement slurries",Proc.3rd Int. Conf. on Concrete under Severe Conditions, Vancouver, June 18-20, 2001.
- (15). Sigurdur Reynir Gislason, Domenik Wolff-Boenisch,Andri Stefansson,Eric H.Oelkers,Einar Gunnlaugsson, Holfridur Sigurdardottir, Bergur Sigfusson,Wallace S.Broecker,Juerg M.Matter,Martin Stute,Gudni Axelsson,Thrainn Fridriksson, "Mineral sequestration of carbon dioxide in basalt:A pre-injection overview of the carbFix project", International journal of greenhousegas control,Elsevier, Vol. 4,2010.
- (16). B.Nelson, Erik."Well cementing",Amsterdam,Elsevier, 1990.
- (17). C.Hewlett, Peter."Lea's chemistry of cement and concrete" Oxford, Elsevier Butterworth-Heinmann, 2004.
- (18). W. S. Dodds, L. F. Stutzman, B. J. Sollami,"Solubility of carbon dioxide in water", Industrial & Engineering Chemistry Research,Vol. 1,1956.
- (19). Wilhelm, Jost."Diffusion in solids, liquids, gases",New York, Academic Press, 1952.

APPENDIX A

PORTLAND CEMENT TYPES

A.1 European Standards (EN 197-1) Portland cement type and composition

EN 197-1 defines and gives the specifications of 27 distinct common cement products and their constituents.

Cement Type	Designation	Notation	Clinker K	G.G.B.S. S	Silica fume D	Pozzolana		Fly ashes		Burnt Shale T	Limestone		Minor Additional constit.
						Natural P	Industrial Q	Silic. V	Calcar W		L	LL	
I	Portland Cement	I	95-100	-	-	-	-	-	-	-	-	-	0-5
II	Portland Slag Cement	II / A-S	80-94	6-20	-	-	-	-	-	-	-	-	0-5
		II / B-S	65-79	21-35	-	-	-	-	-	-	-	-	0-5
	Portland Silica Fume Cement	II / A-D	90-94	-	6-10	-	-	-	-	-	-	-	0-5
	Portland Pozzolana Cement	II / A-P	80-94	-	-	6-20	-	-	-	-	-	-	0-5
		II / B-P	65-79	-	-	21-35	-	-	-	-	-	-	0-5
		II / A-Q	80-94	-	-	-	6-20	-	-	-	-	-	0-5
		II / B-Q	65-79	-	-	-	21-35	-	-	-	-	-	0-5
	Portland Fly Ash Cement	II / A-V	80-94	-	-	-	-	6-20	-	-	-	-	0-5
		II / B-V	65-79	-	-	-	-	21-35	-	-	-	-	0-5
		II / A-W	80-94	-	-	-	-	-	6-20	-	-	-	0-5
Portland Burnt Shale Cement	II / A-W	65-79	-	-	-	-	-	21-35	-	-	-	0-5	
	II / A-T	80-94	-	-	-	-	-	-	6-20	-	-	0-5	
Portland Limestone Cement	II / B-T	65-79	-	-	-	-	-	-	21-35	-	-	0-5	
	II / A-L	80-94	-	-	-	-	-	-	-	6-20	-	0-5	
Portland Composite Cement	II / B-L	65-79	-	-	-	-	-	-	-	21-35	6-20	0-5	
	II / A-LL	80-94	-	-	-	-	-	-	-	-	6-20	0-5	
Portland Composite Cement	II / B-LL	65-79	-	-	-	-	-	-	-	-	21-35	0-5	
	II / A-M	80-94	←-----8-20----->										
Portland Composite Cement	II / B-M	65-79	←-----21-35----->										
	Blastfurnace Cement	III / A	35-64	35-65	-	-	-	-	-	-	-	-	0-5
III / B		20-34	66-80	-	-	-	-	-	-	-	-	0-5	
III / C		5-19	81-95	-	-	-	-	-	-	-	-	0-5	
IV	Pozzolanic Cement	IV / A	65-89	-	←-----11-35----->				-	-	-	0-5	
		IV / B	45-64	-	←-----30-65----->				-	-	-	0-5	
V	Composite Cement	V / A	40-64	18-30	←-----18-30----->				-	-	-	0-5	
		V / B	20-39	31-50	←-----31-50----->				-	-	-	0-5	

Fig A.1 European standards Portland cement type and composition(17)

- D : Silica Fume
- P : Natural Pozzolan
- Q : Calcined Natural Pozzolan
- T : Calcined Shale
- W : Class – C Fly Ash
- V : Class – F Fly Ash
- L : Limestone (Organic compound < 0.5%)
- LL : Limestone (Organic compound < 0.2%)
- S : Granulated Blast Furnace Slag

A.2 American Standards (ASTM C 150) Portland cement type

ASTM C 150 provides eight types of Portland cement to meet various physical and chemical requirements for specific purposes

Table A.1 Type of Portland cement (17)

Type of Portland Cement (ASTM C 150)	Typical Potential compound composition, %				
	C ₃ S	C ₂ S	C ₃ A	C ₄ AF	Blaine fineness (m ² /kg)
I Normal	54	18	10	8	369
II Normal, air-entraining	55	19	6	11	377
III High early strength	57	15	9	8	548
IV Low heat of hydration	42	32	4	15	340
V High sulfate resistance	54	22	4	13	373

Table A.2 Portland cement mechanical and physical requirements (17)

Strength Class Label	Standard 28 day Strength (MPa)		Early Strength (MPa)		Initial Setting Time (min)	Expansion (mm)
			2 days	7 days		
32.5 N	≥ 32.5	≤ 52.5	-		≥ 75	≤ 10.0
32.5 R			≥ 10.0	-		
42.5 N	≥ 42.5	≤ 62.5	≥ 10.0	-	≥ 60	
42.5 R			≥ 20.0	-		
52.5 N	≥ 52.5	-	≥ 20.0	-	≥ 45	
52.5 R			≥ 30.0	-		

Table A.3 Portland cement chemical requirements (17)

Property	Cement Type	Strength Class	Required
Loss on Ignition	CEM I CEM III	All	≤ % 5.0
Insoluble Residue	CEM I CEM III	All	≤ % 5.0
SO ₃	CEM I CEM II CEM IV CEM V	32.5 N 32.5 R 42.5 N	≤ % 3.5
		42.5 R 52.5 N 52.5 R	≤ % 4.0
	CEM III	All	≤ % 4.0
Cl ⁻	All	All	≤ % 0.1

APPENDIX B

OIL WELL CEMENT TYPES

Table B.1 Applications of API classes of cement (16)

API Classification	Mixing Water (gal/sk)	Slurry Weight (lb/gal)	Well Depth (ft)	Static Temperature (°F)
A (Portland)	5.2	15.6	0 to 6,000	80 to 170
B (Portland)	5.2	15.6	0 to 6,000	80 to 170
C (high early)	6.3	14.8	0 to 6,000	80 to 170
D (retarded)	4.3	16.4	6,000 to 12,000	170 to 260
E (retarded)	4.3	16.4	6,000 to 14,000	170 to 260
F (retarded)	4.3	16.4	10,000 to 16,000	230 to 320
G (basic)	5.0	15.8	0 to 8,000	80 to 200
H (basic)	4.3	16.4	0 to 8,000	80 to 200

Table B.2 Ordinary type (O)(16)

Ordinary type (O)	Cement Classes					
	A	B	C	D,E,F	G	H
Magnesium oxide (MgO) maximum, percent	6.00	-	6.00	-	-	-
Sulfur trioxide (SO ₃) maximum, percent	3.50	-	4.50	-	-	-
Loss on ignition maximum, percent	3.00	-	3.00	-	-	-
Insoluble residue maximum, percent	0.75	-	0.75	-	-	-
Tricalcium aluminate (3CaO.Al ₂ O ₃) maximum, percent	-	-	15.00	-	-	-

Table B.3 Moderate sulfate-resistant type (MSR)(16)

Moderate Sulfate-Resistant type (MSR)	Cement Classes					
	A	B	C	D,E,F	G	H
Magnesium oxide (MgO) maximum, percent	-	6.00	6.00	6.00	6.00	6.00
Sulfur trioxide (SO ₃) maximum, percent	-	3.00	3.50	3.00	3.00	3.00
Loss on ignition maximum, percent	-	3.00	3.00	3.00	3.00	3.00
Insoluble residue maximum, percent	-	0.75	0.75	0.75	0.75	0.75
Tricalcium silicate (3CaO.SiO ₂) {max % {min %	- -	- -	- -	- -	58.00 48.00	58.00 48.00
Tricalcium aluminate (3CaO.Al ₂ O ₃) maximum, percent	-	8.00	8.00	8.00	8.00	8.00
Total alkali content expressed as sodium oxide (Na ₂ O) equivalent maximum, percent	-	-	-	-	0.75	0.75

Table B.4 High sulfate-resistant type (HSR) (16)

High Sulfate-Resistant type (HSR)	Cement Classes					
	A	B	C	D,E,F	G	H
Magnesium oxide (MgO) maximum, percent	-	6.00	6.00	6.00	6.00	6.00
Sulfur trioxide (SO ₃) maximum, percent	-	3.00	3.50	3.00	3.00	3.00
Loss on ignition maximum, percent	-	3.00	3.00	3.00	3.00	3.00
Insoluble residue maximum, percent	-	0.75	0.75	0.75	0.75	0.75
Tricalcium silicate (3CaO.SiO ₂) {max % {min %	- -	- -	- -	- -	65.00 48.00	65.00 48.00
Tricalcium aluminate (3CaO.Al ₂ O ₃) maximum, percent	3.00	3.00	3.00	3.00	3.00	3.00
Tetracalciumaluminoferrite(4 CaO.Al ₂ O ₃ .Fe ₂ O ₃) plus twice the tricalcium aluminate (3CaO.Al ₂ O ₃) maximum, percent	-	24.00	24.00	24.00	24.00	24.00
Total alkali content expressed as sodium oxide (Na ₂ O) equivalent maximum, percent	-	-	-	-	0.75	0.75

Table B.5 Physical requirements for API cements (16)

Cement Classes	A	B	C	D	E	F	G	H
Water, percent by weight of cement	46	46	56	38	38	38	44	38
Soundness(autoclave expansion) Max (%)	0.8	0.8	0.8	0.8	0.8	0.8	0.8	0.8
Fineness (Specific Surface) Min (m ² /kg)	150	160	220	-	-	-	-	-
Free water content Max (ml)	-	-	-	-	-	-	3.5	3.5

Table B.6 Minimum compressive strength after 8 h curing time (16)

Cement Classes		A	B	C	D	E	F	G	H
Curing temperature	Curing Pressure	Minimum Compressive Strength MPa(ψ) after <u>8 h</u> curing time							
°C (°F)	KPa (ψ)								
38 (100)	Atmospheric	1.7 (250)	1.4 (200)	2.1 (300)	–	–	–	2.1 (300)	2.1 (300)
60 (140)	Atmospheric	–	–	–	–	–	–	10.3 (1500)	10.3 (1500)
110 (230)	20700 (3000)	–	–	–	3.5 (500)	–	–	–	–
143 (290)	20700 (3000)	–	–	–	–	3.5 (500)	–	–	–
160 (320)	20700 (3000)	–	–	–	–	–	3.5 (500)	–	–

Table B.7 Minimum compressive strength after 24 h curing time (16)

Cement Classes		A	B	C	D	E	F	G	H
Curing temperature	Curing Pressure	Minimum Compressive Strength MPa(ψi) after <u>24 h</u> curing time							
°C (°F)	KPa (ψi)								
38 (100)	Atmospheric	12.4 (1800)	10.3 (1500)	13.8 (2000)	–	–	–	–	–
77 (170)	20700 (3000)	–	–	–	6.9 (1000)	6.9 (1000)	–	–	–
110 (230)	20700 (3000)	–	–	–	13.8 (2000)	–	6.9 (1000)	–	–
143 (290)	20700 (3000)	–	–	–	–	13.8 (2000)	–	–	–
160 (320)	20700 (3000)	–	–	–	–	–	6.9 (1000)	–	–

APPENDIX C

MIXING DEVICES FOR PREPARATION OF CEMENT PLUGS

The mixing devices for preparation of well cement slurries are one liter or (one quart) size, bottom-drive, blade type mixer.

Example of mixing devices in common use are shown in Figure C.1. The mixing blade and mixing container shall be constructed of durable corrosion-resistant material. The mixing assembly shall be constructed in such a manner that the blade can be removed for weighting and changing. The mixing blade shall be weighted prior to use and replaced with an unused blade when 10% mass loss has occurred. If water leakage occurs around the bearings, the entire blender blade assembly should be replaced.

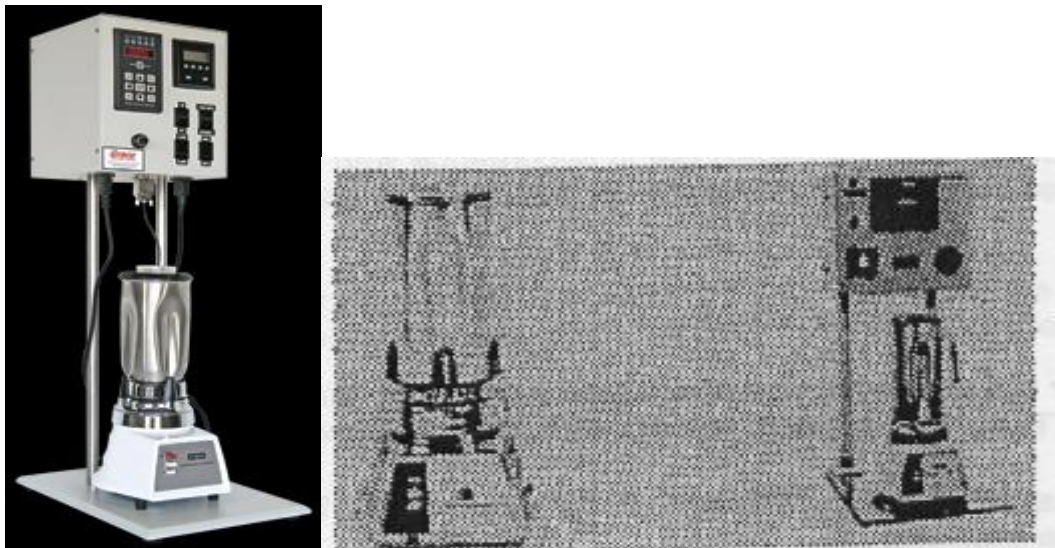


Fig C.1 Examples of typical cement mixing device

C.1 Procedures

Prior the mixing, cement is sieved as described in ASTM C183.

C.1.1 Temperature of water and cement

The temperature of mixed water in the container within 60 S before mixing is $23\text{ }^{\circ}\text{C} \pm 1\text{ }^{\circ}\text{C}$ ($73\text{ }^{\circ}\text{F} \pm 2^{\circ}\text{F}$) and that of the cement within 60 s prior the mixing is $23\text{ }^{\circ}\text{C} \pm 1\text{ }^{\circ}\text{C}$ ($73\text{ }^{\circ}\text{F} \pm 2^{\circ}\text{F}$).

C.1.2 Mix water

Distilled or deionized water are used for testing. The mix water shall be weighted directly into clean, dry mixing container. no water will be added to compensate for evaporation, wetting, etc.

C.1.3 Mixing quantities

Slurry component quantities shown in table C.1 is used for testing. The use of the quantities of component shown in this table will result in mix water percentages. (Based on the mass of the dry cement).

Table C.1 Slurry component quantities

Components	Class A,B	Class C	Class D,E,F,H	Class G
Mix water, g	355±0,5	383±0,5	327±0,5	349±0,5
Cement, g	772±0,5	684±0,5	860±0,5	792±0,5

C.1.4 Mixing cement and water

The mixing container with required mass of mixed water as given in table C.1 shall be placed on the mixer base, the motor turned on and maintained at $4000\text{ rpm} \pm 200\text{ rpm}$ ($66,7\text{ r/s} \pm 3,3\text{ r/s}$) while the cement sample is added at a uniform rate in not more than 15s. after all of the cement has been added to the mix water, the cover shall be placed on the mixing container and mixing shall be continued at $12000\text{ r/min} \pm 500\text{ r/min}$ ($200\text{ r/s} \pm 8,3\text{ r/s}$) for $35\text{ seconds} \pm 1\text{ second}$.

APPENDIX D

PHOTOGRAPHS OF CEMENT PLUGS AND EXPERIMENTAL SET UP



FigD.1 Photograph of 4 samples



Fig D.2 Photograph of 4 cement plugs with different compositions before 90 days



Fig D.3 Photograph of 4 cement plugs with four core holders



Fig D.4 Photograph of experimental set up

APPENDIX E

COMPARISON GRAPHS OF THE ELEMENT CONCENTRATIONS IN CO₂-WATER MIX AND FOUR CEMENT PLUGS

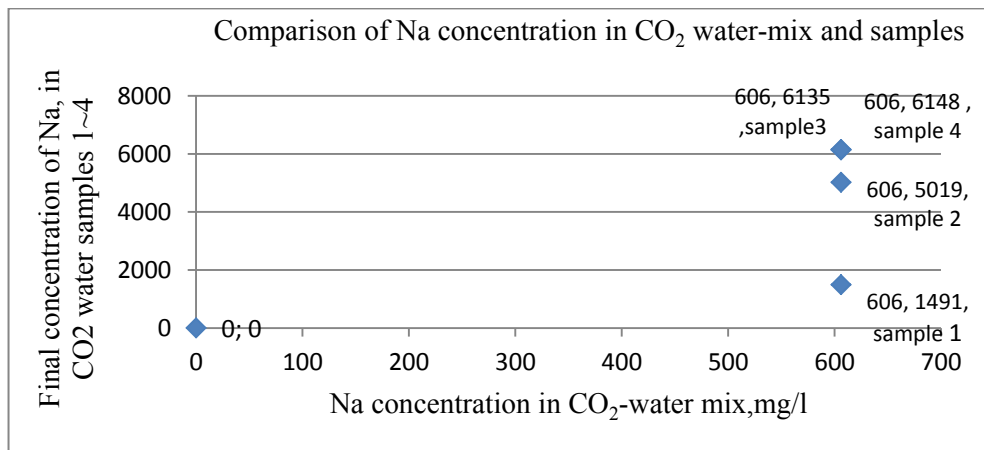


Fig E.1 Na concentration variation in water from sample 1~4

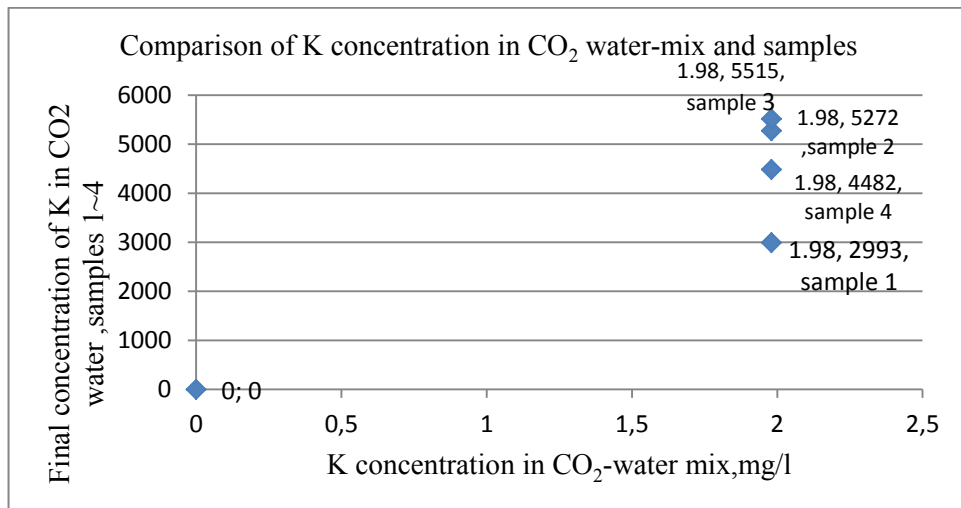


Fig E.2 K concentration variation in water from sample 1~4

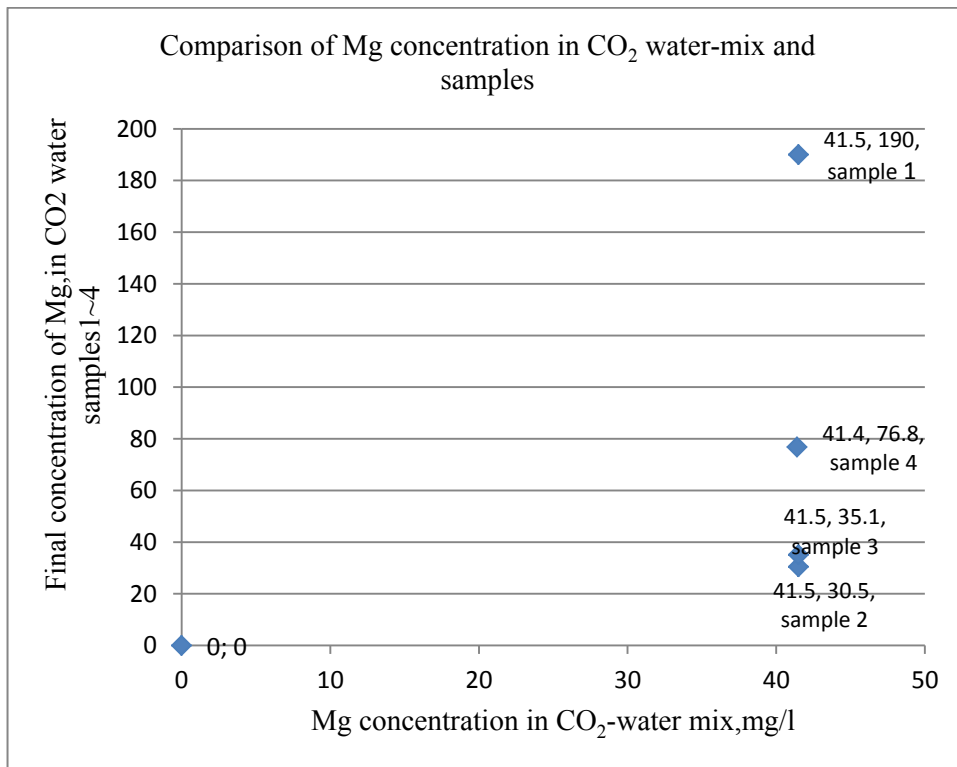


Fig E.3 Mg concentration variation in water from sample 1~4

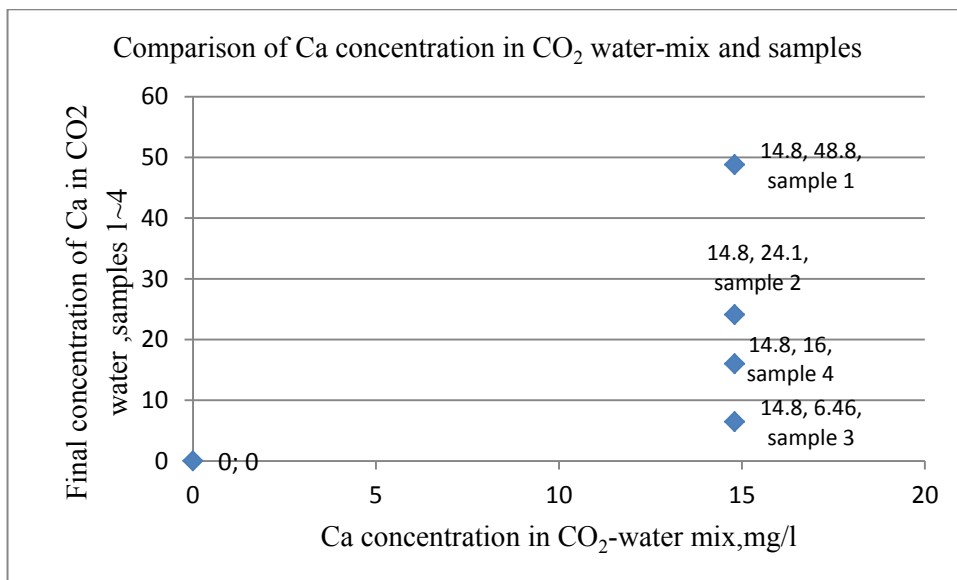


Fig E.4 Ca concentration variation in water from sample 1~4

APPENDIX F

POROSITY AND PERMEABILITY MEASUREMENT APPARATUS OF CEMENT PLUGS ACCORDING TO THE API RP 40

F.1 Boyle's law double-cell method for grain volume (Porosity Determination)

F.1.2 Apparatus and Procedure

The grain volume is measured in an apparatus consisting of two connected chambers of known volume. An example of such apparatus is shown in figure F.1.

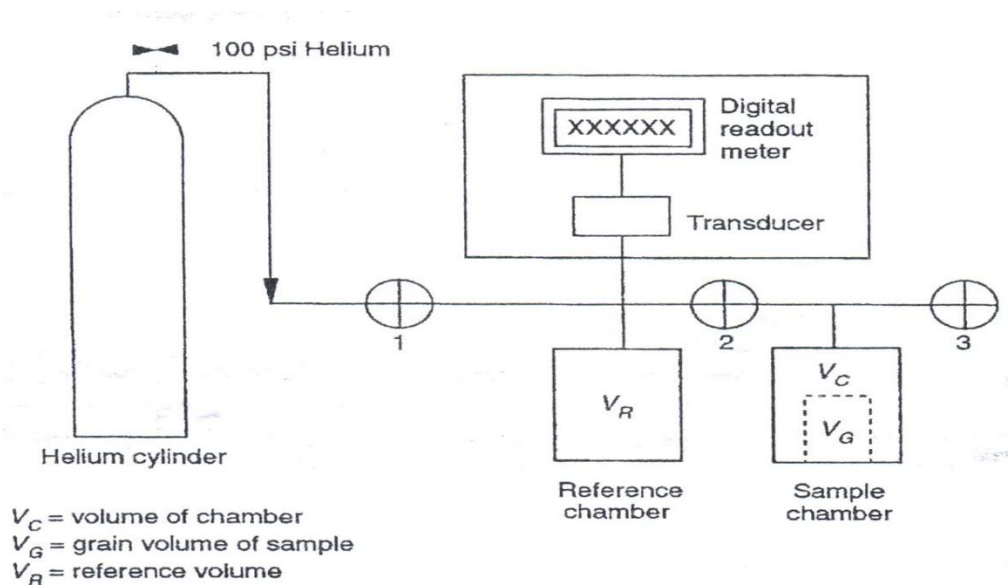


Fig F.1 Double-Cell Boyle's Law Porosimeter

F.2 Boyle's law single cell method for direct pore volume

Pore volume is determined in an apparatus consisting of gas charged reference cell of known volume and initial pressure, which is then vented into a sample's pore volume.

F.2.1 Apparatus and Procedure

The basic apparatus shown in figure F.2 is the same as that illustrated for the double-cell Boyle's law porosimeter shown in figure F.1. The primary difference is the design of the sample chamber, which eliminates volume around the periphery of the sample. The porosity measurements of cement plugs before and after experiment are given in table F.1.

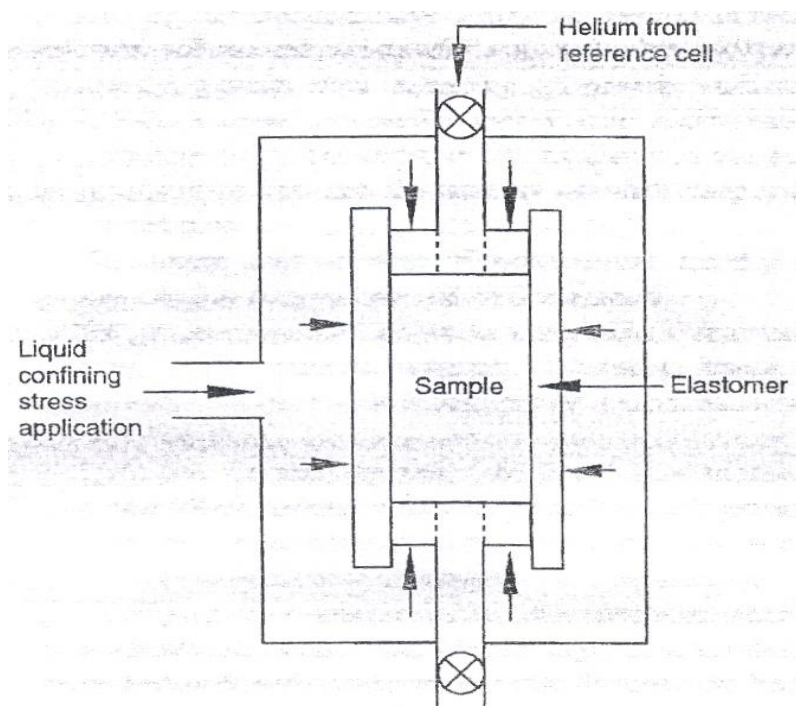


Fig F.2 Schematic of isostatic load cell for direct pore volume determination

Table F.1 Porosity measurement of cement plugs before and after experiment

Sample ID	Sample dia (mm)	Sample Length (mm)	Bulk Vol (cc)	Weight (g)	Grain Volume (cc)	Pore Volume (cc)	Grain density (g/cc)	Core Porosity (%)	Pref (psi)	Pexp (psi)	Pratio
1b	23.41	46.70	20.10	33.69	13.94	6.16	2.42	30.65%	99.53	71.33	1.40
2b	23.25	46.70	19.83	33.82	14.05	5.78	2.41	29.15%	100.3	73.06	1.37
3b	23.35	47.80	20.47	36.26	14.88	5.59	2.44	27.31%	100.4	72.78	1.38
4b	23.35	28.00	11.99	21.51	8.72	3.27	2.47	27.27%	100.3	76.00	1.32
1a	*	*	*	17.59	7.51	-7.51	2.34	*	100.3	74.84	1.34
2a	25.1	47.40	23.45	47.19	18.22	5.23	2.59	22.30%	100.4	75.87	1.32
3a	25.10	50.90	25.19	30.86	20.48	4.71	1.51	18.70%	100.3	76.90	1.31
4a	25.45	31.60	16.08	42.28	13.27	2.81	3.19	17.48	100.3	79.37	1.26

b: Before experiment

a: After experiment

* In sample 1 because of the sample broke while dismantling from core holder porosity value was not determined.

F.3 Axial, Steady-State flow of gases (Permeability determination)

A schematic arrangement for axial flow of gases is shown in figure F.3. A cleaned and dried cylindrical core plug or whole cement plug of length L and diameter D is mounted in a sample holder. The holder contains a flexible sleeve for purposes of making a gas-tight seal on the cylindrical walls of the sample, and for applying radial confining stresses. Axial stress can be transmitted to the sample by applying force to one or both end plugs, by mechanical, pneumatic, or hydraulic means. If the magnitude of the radial and axial stresses is equal, the sample is said to be isotastically or hydrostatically stressed. If the magnitudes are unequal, the sample is biaxially stressed. When gases at relatively low pressures (up to a few hundred psig) are used, gravity effects are negligible, and the sample holder may be oriented either horizontally or vertically. The two end plugs are provided with an axial port for transporting gas to and from the sample, each should have radial and circular grooves or other means for distributing gas to its entire injection face, and for collecting gas from all parts of its outflow face. Each end plug, preferably, also contains a second port for measuring upstream and downstream pressures, P_1 and P_2 , respectively; the upstream pressure and differential pressure, ΔP , as illustrated in figure F.3; or the

differential and downstream pressures. However, lines for connecting the pressure-measuring devices can be teed into the flow lines near the axial ports, provided that the latter are sufficiently large not to cause significant pressure drops between each tee and the corresponding end face of the sample.

It is essential that the branch of each tee (not the run) is connected to the pressure transducer. otherwise, dynamic pressure effects may influence the pressure measurements.

Note that ΔP , as used throughout this document is always a positive number, therefore is equal to $P_1 - P_2$ or to $p_1 - p_2$. As indicated previously, an upper case P denotes an absolute pressure, and a lower case p, a gauge or differential pressure. The outflow line can be vented directly to the atmosphere pressure (when the flow meter is upstream of the sample), connected to the flow rate measuring device, or to a back pressure regulator for purpose of creating elevated mean pore pressures. in the latter case, the flow meter can be either upstream of the sample or downstream of the back pressure regulator. The volumetric flow rate, q_r , can be measured at the upstream and downstream pressure, or some other pressure, which in all cases is denoted as P_r , an absolute pressure. The temperature at which the flow rate is measured is assumed to be the same as the flowing gas temperature. Alternatively, the group $(q_r, P_r) / (Z_r, T_r)$, which is proportional to mass flow rate, can be determined by a mass flow meter. The permeability measurements of cement plugs before and after experiment are given in table F.2.

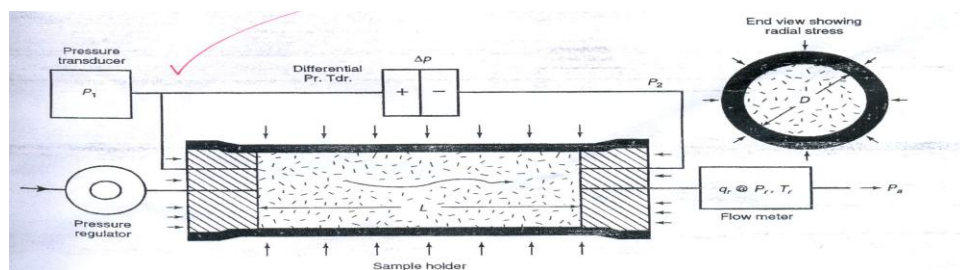


Fig F.3 Schematic of Permeability Apparatus for Axial Flow of Gas

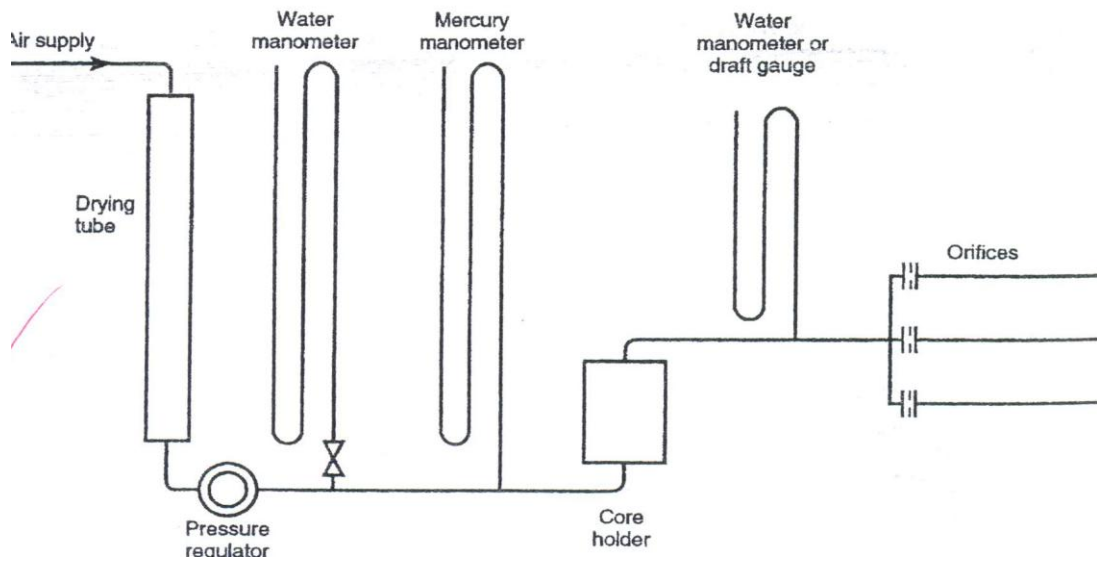


Fig F.4 Simplified Flow Diagram for Low Pressure, Axial gas Flow Permeability Measurement

Table F.2 Permeability measurements of cement plugs before and after experiment

Sample Name	Dia (mm)	Length (mm)	Atm. Press. (psi)	Confining Pressure Radial (psig)	Upstream P. (psig)	DP (psid)	Temp (°C)	Low flow (Ncc/min)	High flow (Ncc/min)	Ka(mD)
1b	23.41	46.70	13.43	300	85.59	-0.010	22.0	2.213	-2.4	0.035
2b	23.25	46.70	13.43	300	85.79	-0.011	22.1	0.618	-2.4	0.010
3b	23.35	47.80	13.43	300	85.84	-0.011	22.3	1.556	-2.4	0.025
4b	23.35	28.00	13.43	300	85.91	-0.012	22.4	0.897	-2.4	0.009
1a	*	*	*	*	*	*	*	*	*	*
2a	25.10	47.40	13.43	300	85.97	-0.012	22.6	-1.218	-2.4	-0.017
3a	25.10	50.90	13.43	300	85.30	-0.014	23.2	-1.973	-2.5	-0.030
4a	25.45	31.60	13.43	300	85.83	-0.013	22.8	-2.049	88.4	*

b: Before experiment
a: After experiment

*In sample 1 and 4 because of the sample broke while dismantling from core holder permeability values was not determined.

APPENDIX G

AP-1000 VERSA-TESTER APPARATUS FOR MEASURING THE COMPRESSIVE STRENGTH OF SAMPLES

The Ap-1000 Series Versa-Tester is a hydraulically-operated testing machine for testing materials of all types up to load ranges of 30,000 and 60,000 pounds. Gauges in other load capacities can also be supplied on special order. Two 8 1/2" diameter gauges of full and 1/5 capacity are supplied. The Versa-Tester may also be adapted to tension testing.

Each Versa-Tester is individually calibrated using U.S. Bureau of Standards certified proving rings. A calibration certificate is furnished with each testing machine. A pressure relief valve (pre-set to gauge capacity) is installed in each machine to prevent overloading of the pressure gauges. Figure G.1 shows the schematic of the Versa-Tester apparatus



Fig G.1 Schematic of Versa-Tester Apparatus

APPENDIX H

PHOTOGRAPHS OF CEMENT PLUGS AFTER THE 90 DAYS EXPERIMENT



Fig H.1 Photograph of cement plugs after experiment



Fig H.2 Photograph of cement plug # 1 after experiment



Fig H.3 Photograph of cement plug # 2 after experiment



Fig H.4 Photograph of cement plug# 3 after experiment



Fig H.5 Photograph of cement plug # 4 after experiment

APPENDIX I

SEM/EDS ANALYSIS OF FOUR CEMENT PLUGS BEFORE AND AFTER EXPERIMENT

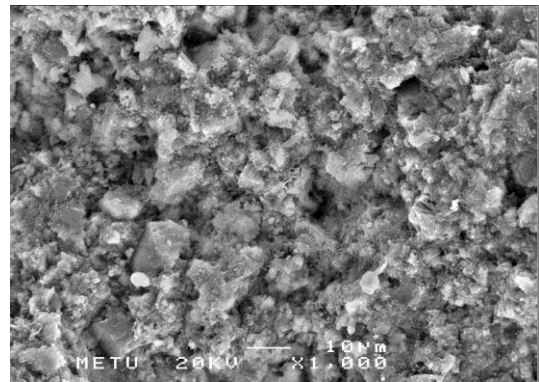
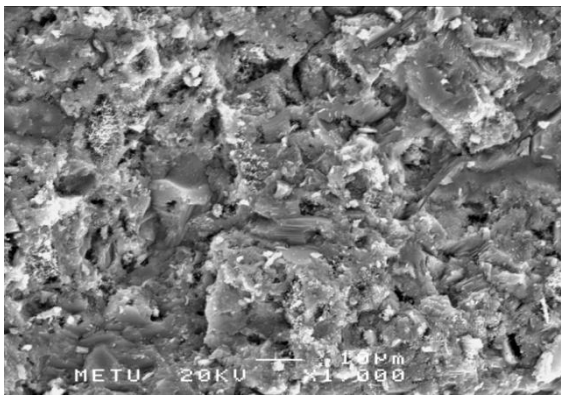


Fig I.1 Near to surface view of sample # 1 (before EXP) **Fig I.2** Near to surface view of sample #1 (after EXP)

Table I.1Element analysis of near to surface of sample # 1 (before EXP)

Element	Weight Conc %	Atom Conc %
Mg	0.75	1.16
Al	2.40	3.34
Si	15.30	20.49
K	1.07	1.03
Ca	74.68	70.08
Fe	5.81	3.91

Table I.2Element analysis of near to surface of sample # 1 (after EXP)

Element	Weight Conc %	Atom Conc %
Mg	0.28	0.45
Al	2.59	3.65
Si	15.07	20.39
K	1.86	1.80
Ca	71.65	67.90
Fe	8.55	5.81

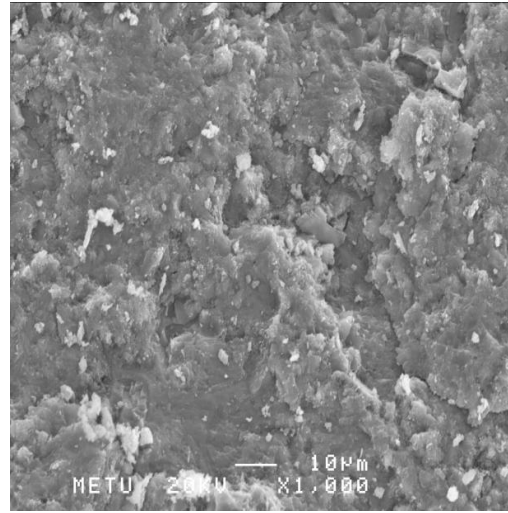
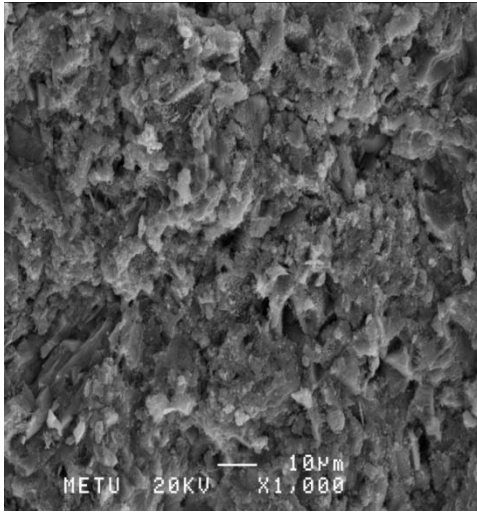


Fig I.3 Near to surface view of sample # 2 (before EXP) **Fig I.4** Near to surface view of sample #2 (after EXP)

Table I.3 Element analysis of near to surface of sample# 2 (before EXP)

Element	Weight Conc %	Atom Conc %
Mg	0.43	0.66
Al	1.91	2.68
Si	14.76	19.86
K	1.23	1.19
Ca	76.35	72.00
Fe	5.33	3.61

Table I.4 Element analysis of near to surface of sample # 2 (after EXP)

Element	Weight Conc %	Atom Conc %
Mg	0.47	0.71
Al	3.07	4.18
Si	21.05	27.52
K	2.97	2.79
Ca	66.37	60.81
Fe	6.07	3.99

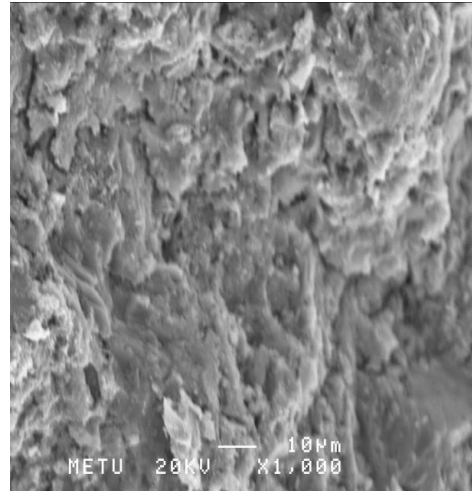
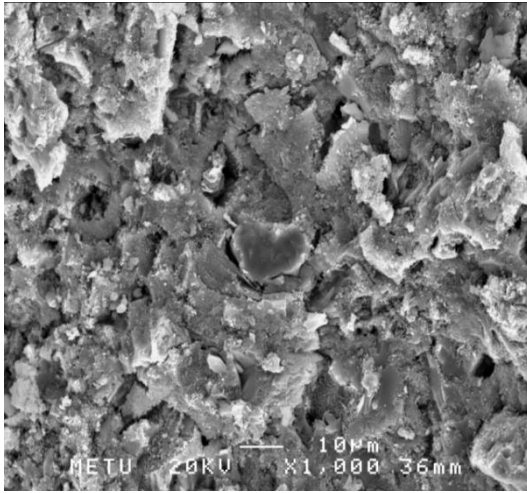


Fig I.5 Near to surface view of sample #3 (before EXP) **Fig I.6** Near to surface view of sample #3 (after EXP)

Table I.5 Element analysis of near to surface sample # 3 (before EXP) **Table I.6** Element analysis of near to surface of sample# 3 (after EXP)

Element	Weight Conc %	Atom Conc %	Element	Weight Conc %	Atom Conc %
Mg	0.67	1.02	Mg	0.45	1.02
Al	2.50	3.44	Al	2.13	3.44
Si	18.05	23.86	Si	14.46	23.86
K	2.77	2.63	K	1.13	2.63
Ca	70.80	65.58	Ca	72.80	65.58
Fe	5.21	3.47	Fe	5.61	3.47

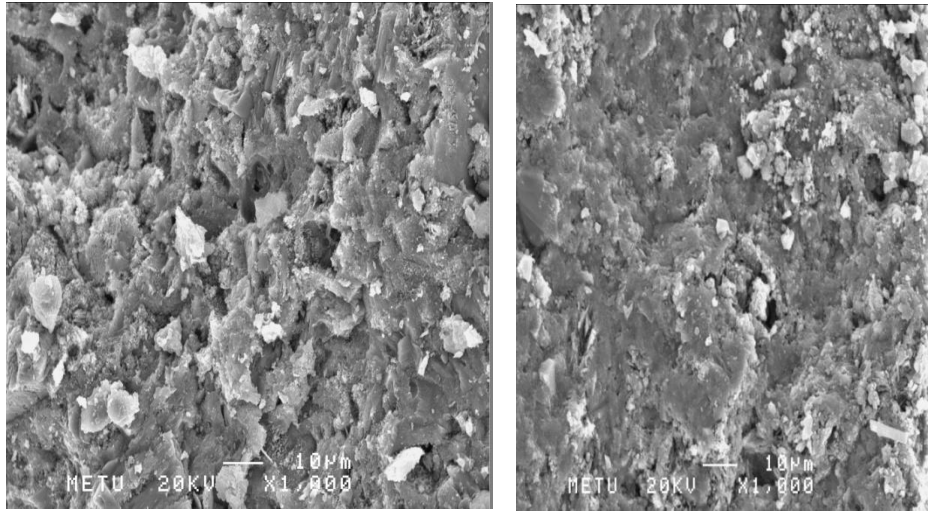


Fig I.7 Near to surface view of sample # 4 (before EXP) **Fig I.8** Near to surface view of sample # 4 (after EXP)

Table I.7 Element analysis of near to surface of sample# 4 (before EXP)

Element	Weight Conc %	Atom Conc %
Mg	0.40	0.62
Al	3.46	4.81
Si	15.72	21.01
K	1.53	1.47
Ca	72.15	67.56
Fe	6.74	4.53

Table I.8 Element analysis of near to surface of sample # 4 (after EXP)

Element	Weight Conc %	Atom Conc %
Mg	0.82	1.25
Al	3.03	4.15
Si	14.05	18.47
K	3.84	3.63
Ca	70.94	65.37
Fe	4.89	3.23

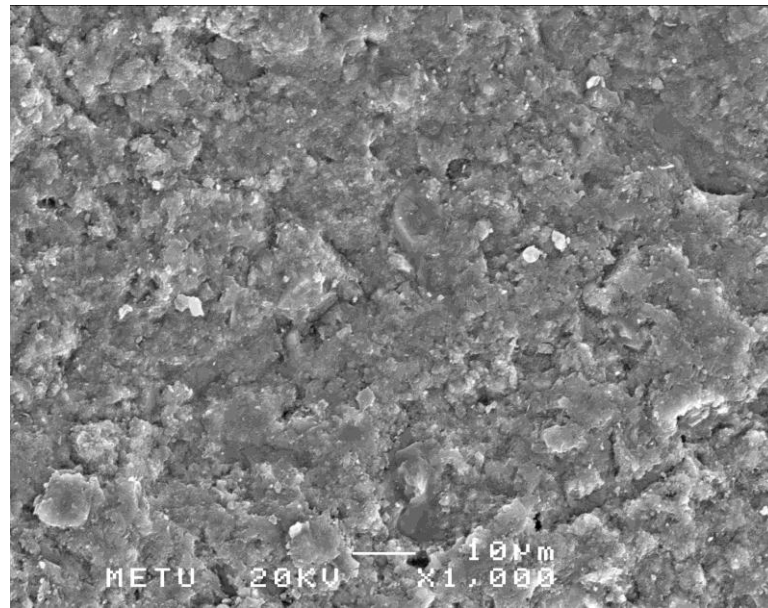


Fig I.9 Inner view of in depth SEM analysis for sample # 1 (after EXP)

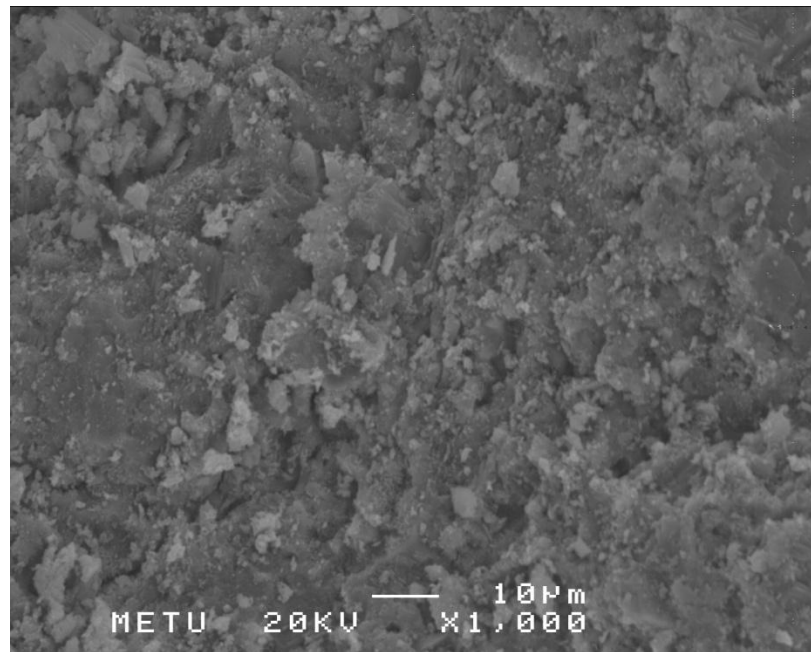


Fig I.10 Inner view of in depth SEM analysis for sample # 2 (after EXP)

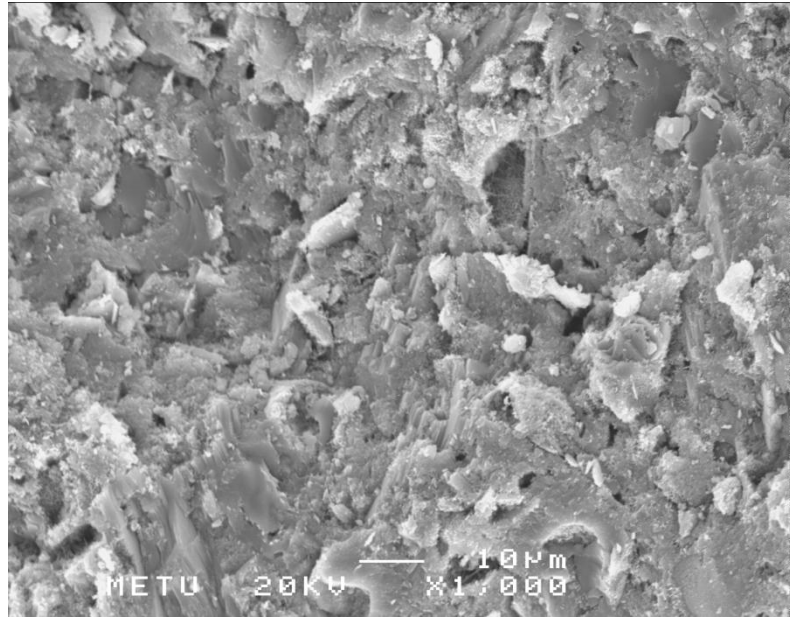


Fig I.11 Inner view of in depth SEM analysis for sample # 3 (after EXP)

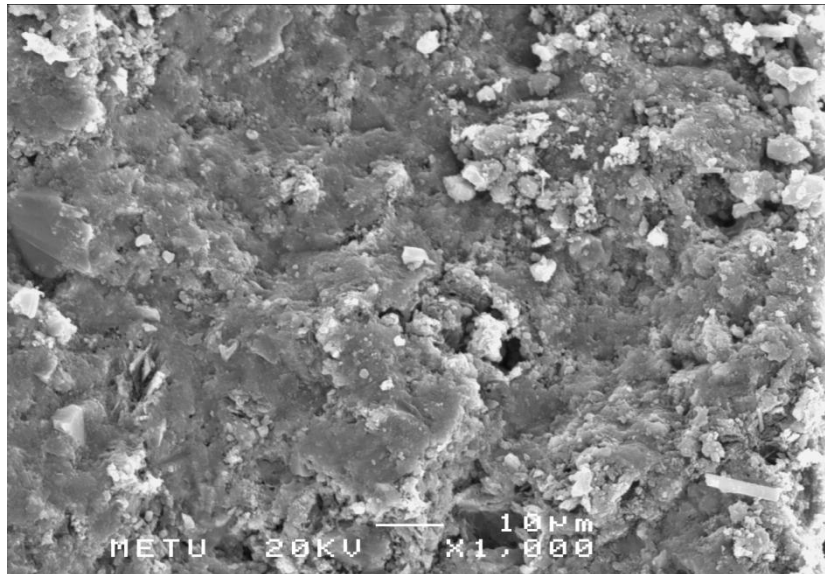


Fig I.12 Inner view of in depth SEM analysis for sample # 4 (after EXP)

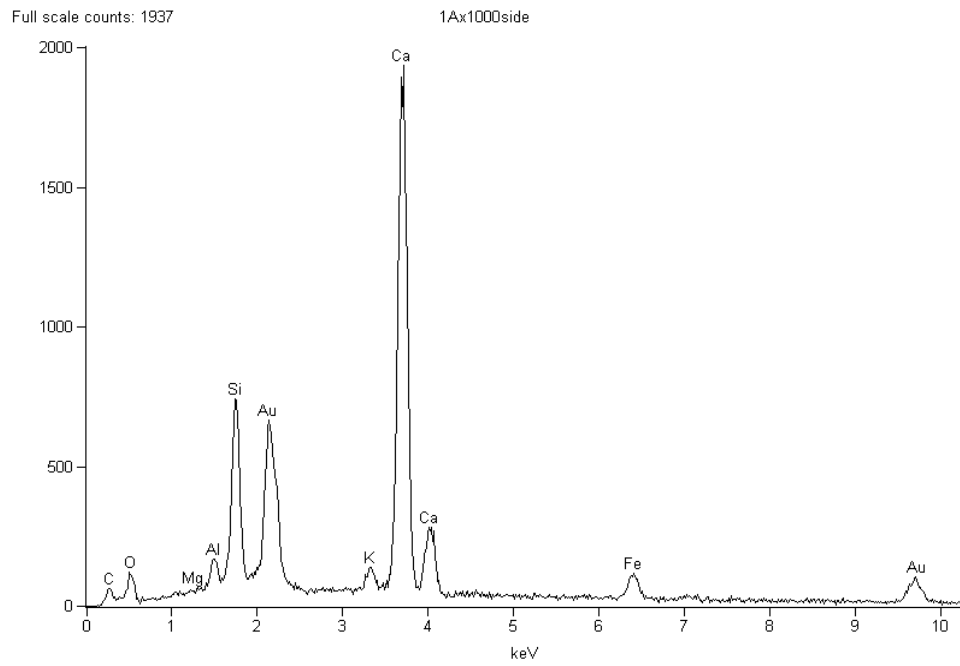


Fig I.13 SEM/EDS micrograph of near surface of sample # 1 (after EXP)

Table I.9 SEM/EDS element analysis of near to surface for sample #1(after EXP)

<i>Element</i>	<i>Weight Conc %</i>	<i>Atom Conc %</i>
<i>Mg</i>	0.28	0.45
<i>Al</i>	2.59	3.65
<i>Si</i>	15.07	20.39
<i>K</i>	1.86	1.80
<i>Ca</i>	71.65	67.90
<i>Fe</i>	8.55	5.81

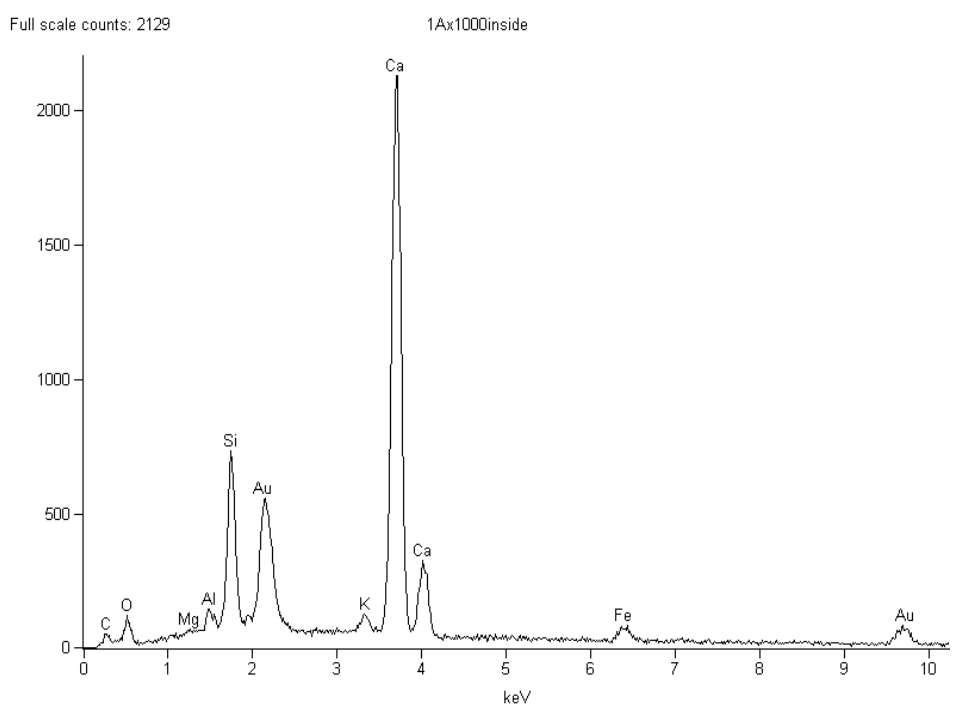


Fig I.14 SEM/EDS micrograph for inner section of sample # 1(after EXP)

Table I.10 SEM/EDS element analysis for inner section of sample # 1(after EXP)

<i>Element</i>	<i>Weight Conc %</i>	<i>Atom Conc %</i>
<i>Mg</i>	0.66	0.03
<i>Al</i>	1.76	2.48
<i>Si</i>	13.23	17.88
<i>K</i>	1.82	1.77
<i>Ca</i>	77.50	73.42
<i>Fe</i>	8.55	3.42

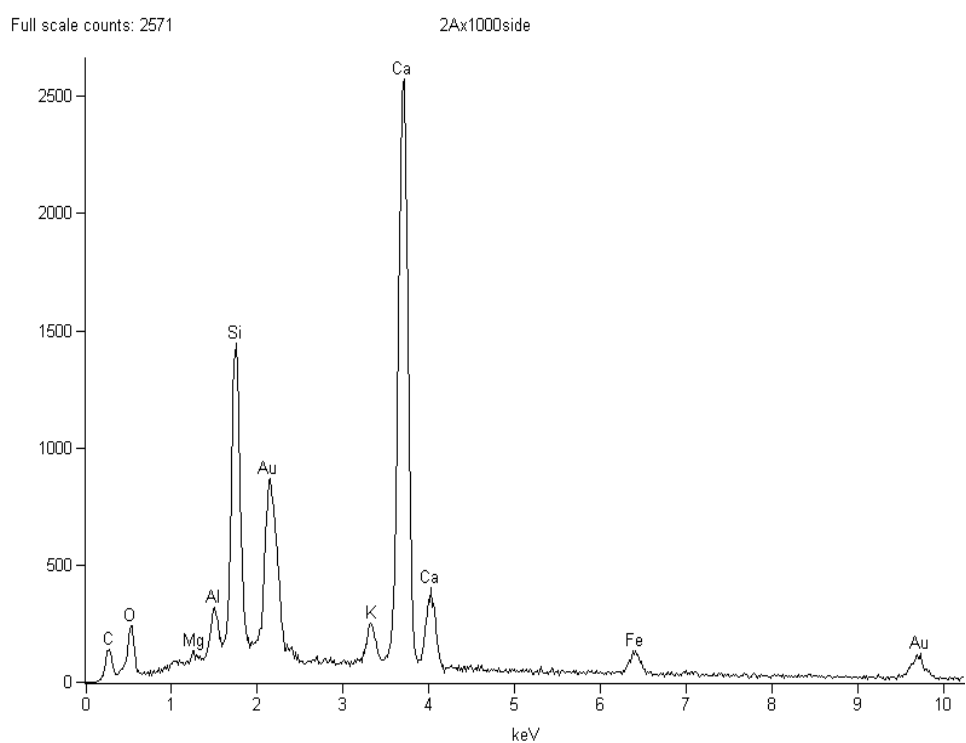


Fig I.15 SEM/EDS micrograph of near surface of sample # 2 (after EXP)

Table I.11 SEM/EDS element analysis of near to surface for sample #2(after EXP)

<i>Element</i>	<i>Weight Conc %</i>	<i>Atom Conc %</i>
<i>Mg</i>	0.47	0.71
<i>Al</i>	3.07	4.18
<i>Si</i>	21.05	27.52
<i>K</i>	2.97	2.79
<i>Ca</i>	66.37	60.81
<i>Fe</i>	6.07	3.99

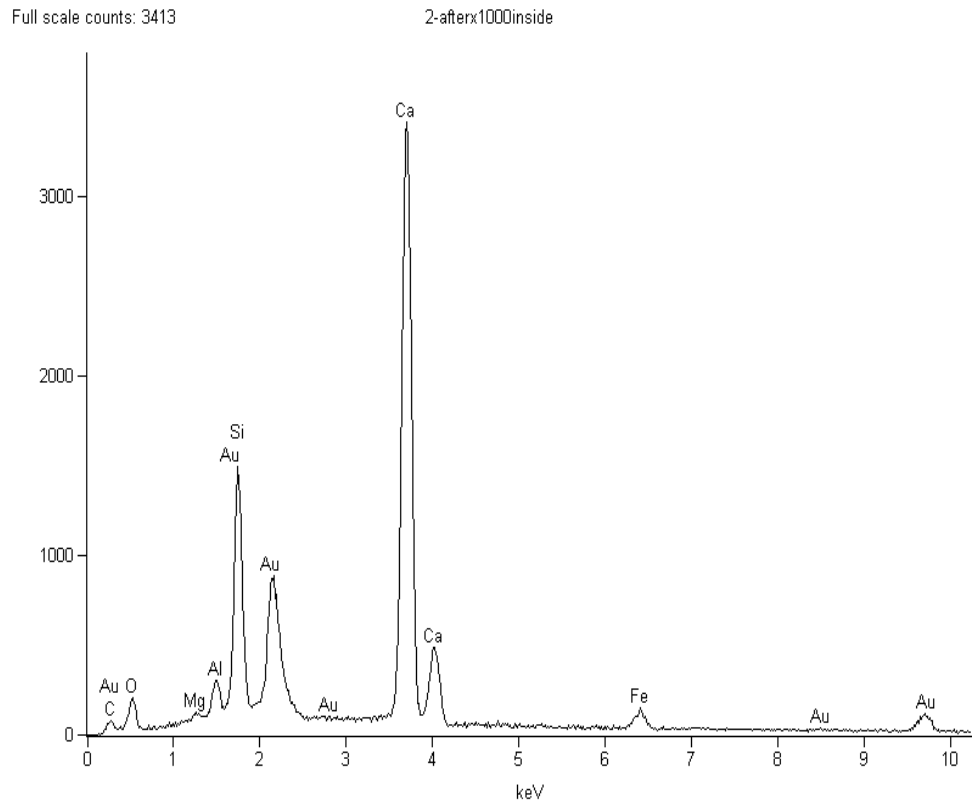


Fig I.16 SEM/EDS micrograph for inner section of sample# 2(after EXP)

Table I.12 SEM/EDS element analysis for inner section of sample 2#(after EXP)

<i>Element</i>	<i>Weight Conc %</i>	<i>Atom Conc %</i>
<i>Mg</i>	0.60	0.92
<i>Al</i>	2.56	3.54
<i>Si</i>	17.55	23.29
<i>Ca</i>	73.69	68.51
<i>Fe</i>	5.60	3.74

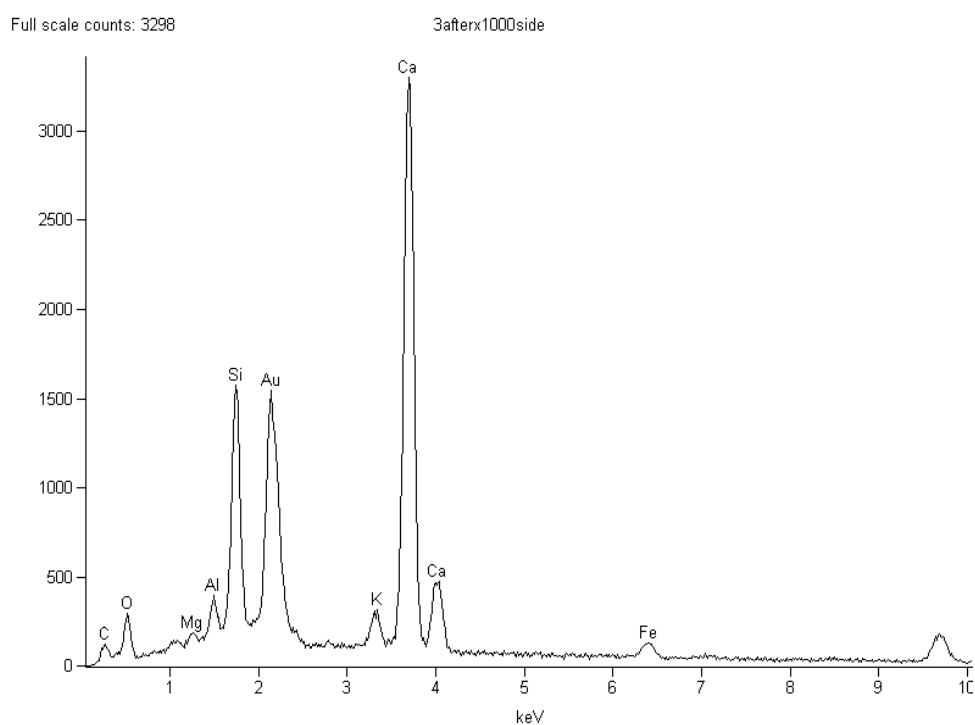


Fig I.17 SEM/EDS micrograph of near surface of sample # 3(after EXP)

Table I.13 SEM/EDS element analysis of near to surface for sample # 3(after EXP)

<i>Element</i>	<i>Weight Conc %</i>	<i>Atom Conc %</i>
<i>Mg</i>	0.67	1.02
<i>Al</i>	2.50	3.44
<i>Si</i>	18.05	23.86
<i>K</i>	2.77	2.63
<i>Ca</i>	70.80	65.58
<i>Fe</i>	5.21	3.47

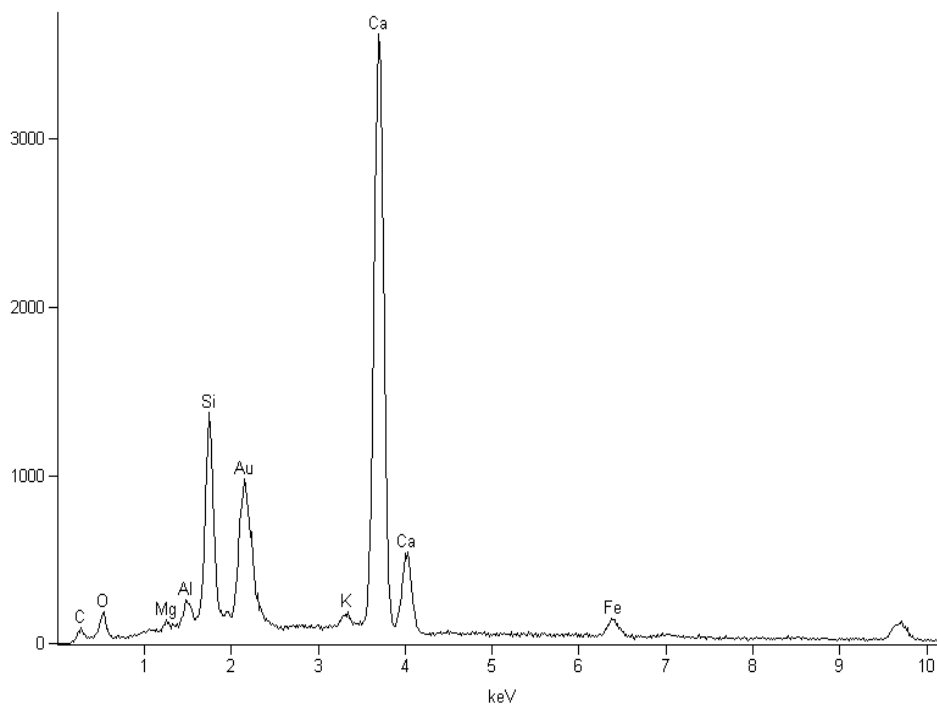


Fig I.18 SEM/EDS micrograph for inner section of sample# 3(after EXP)

Table I.14 SEM/EDS element analysis for inner section of sample #3(after EXP)

<i>Element</i>	<i>Weight Conc %</i>	<i>Atom Conc %</i>
<i>Mg</i>	1.02	1.58
<i>Al</i>	2.23	3.10
<i>Si</i>	14.84	19.88
<i>K</i>	1.32	1.27
<i>Ca</i>	74.81	70.26
<i>Fe</i>	5.79	3.90

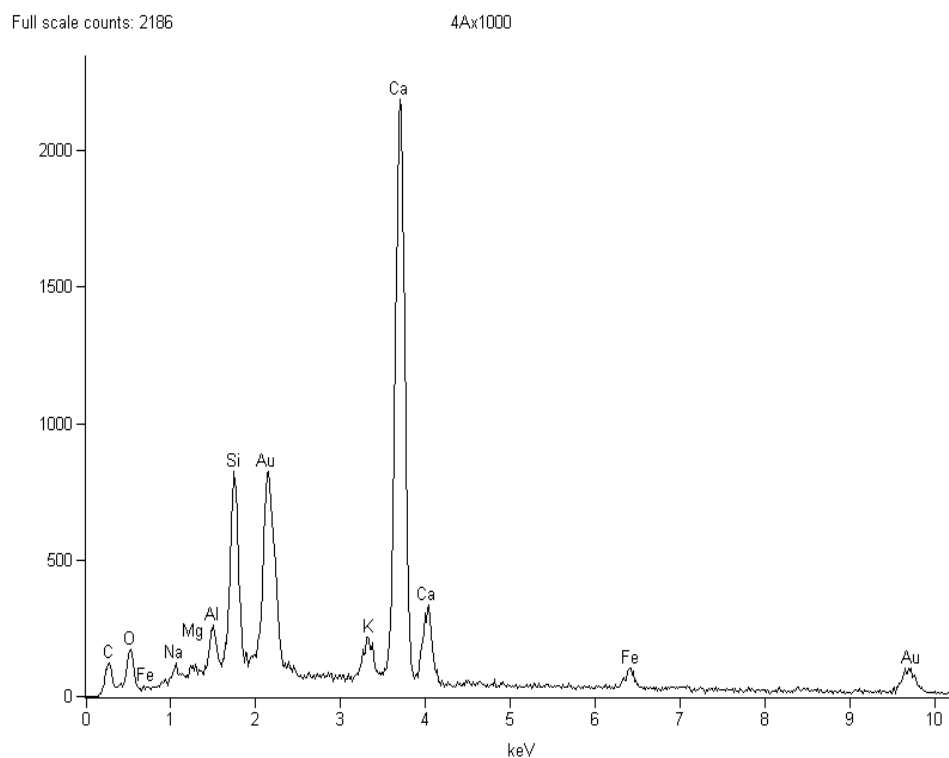


Fig I.19 SEM/EDS micrograph of near surface of sample# 4(after EXP)

Table I.15 SEM/EDS element analysis of near to surface for sample #4(after EXP)

<i>Element</i>	<i>Weight Conc %</i>	<i>Atom Conc %</i>
<i>Mg</i>	0.82	1.25
<i>Al</i>	3.03	4.15
<i>Si</i>	14.05	18.47
<i>K</i>	3.84	3.63
<i>Ca</i>	70.94	65.37
<i>Fe</i>	4.89	3.23

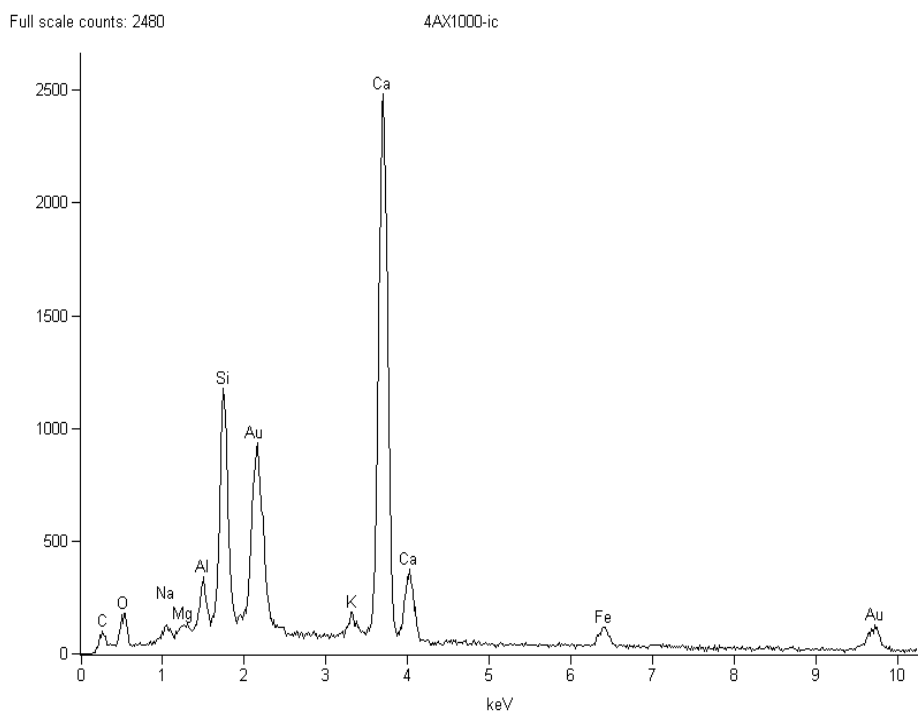


Fig I.20 SEM/EDS micrograph for inner section of sample# 4(after EXP)

Table I.16 SEM/EDS element analysis for inner section of sample # 4(after EXP)

<i>Element</i>	<i>Weight Conc %</i>	<i>Atom Conc %</i>
<i>Mg</i>	1.29	1.91
<i>Al</i>	4.16	5.57
<i>Si</i>	18.07	23.25
<i>K</i>	1.81	1.67
<i>Ca</i>	66.54	60.00
<i>Fe</i>	5.63	3.64